Journal Pre-proofs

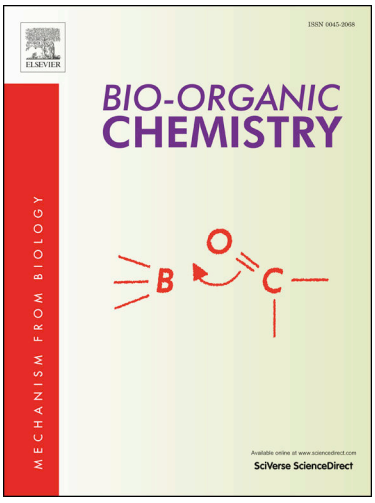

Synthesis and biological evaluation of 2-*epi*-jaspine B analogs as selective sphingosine kinase 1 inhibitors

Haoran Yang, Ying Li, Huining Chai, Takayuki Yakura, Bo Liu, Qingqiang Yao

PII: S0045-2068(19)31138-1
DOI: https://doi.org/10.1016/j.bioorg.2019.103369
Reference: YBIOO 103369

To appear in: *Bioorganic Chemistry*

Received Date: 18 July 2019
Revised Date: 4 October 2019
Accepted Date: 14 October 2019

Please cite this article as: H. Yang, Y. Li, H. Chai, T. Yakura, B. Liu, Q. Yao, Synthesis and biological evaluation of 2-*epi*-jaspine B analogs as selective sphingosine kinase 1 inhibitors, *Bioorganic Chemistry* (2019), doi: https://doi.org/10.1016/j.bioorg.2019.103369

Graphical Abstract

A tetrahydropyrrolidine analog **YHR17,** which was obtained using structural transformation and modification of 2-*epi*-jaspine B, inhibited SphK1 with more than 125-fold selectivity over SphK2. This analog demonstrated potent antiproliferative activities with IC_{50} values ranging from 0.68 to 5.68 μM against tested cancer cell lines and inhibited proliferation of the A375 cell line by affecting cell cycle and apoptosis.

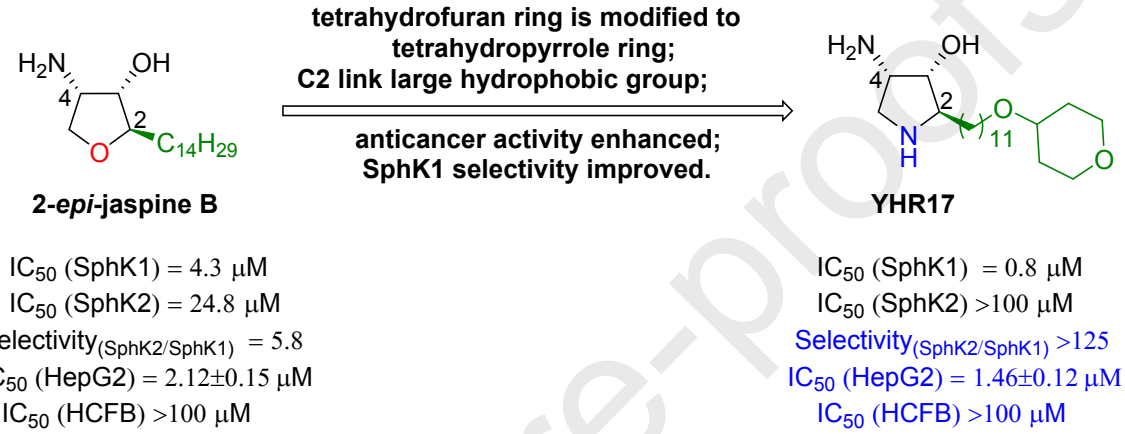

Title page

Title:

Synthesis and biological evaluation of 2-*epi*-jaspine B analogs as selective sphingosine kinase 1 inhibitors

Author names and affiliations:

Haoran Yang[1,2,3#], Ying Li[1,2,3#], Huining Chai[1,2,3], Takayuki Yakura[4], Bo Liu[1,2,3]*, Qingqiang Yao[1,2,3]*

[1]Institute of Materia Medica, Shandong Academy of Medical Sciences, Jinan 250062, P. R. China; [2]Key Laboratory for Biotech-Drugs Ministry of Health, Jinan 250062, P. R. China; [3]Key Laboratory for Rare & Uncommon Diseases of Shandong Province, Jinan 250062, P. R. China; [4]Graduate School of Medicine and Pharmaceutical Sciences, University of Toyama, Toyama 930-0194, Japan.

* Corresponding address:

Tel.: +86-531-82919962; E-mail: mls_liub@ujn.edu.cn; yao_imm@163.com

[#]: These authors contributed equally.

Abstract:

2-*Epi*-jaspine B is an isomer of the natural product jaspine B and shows certain selectivity for SphK1 and potent antitumor activity. Based on the crystal structure of SphK1, we transformed the structure of 2-*epi*-jaspine B and modified the hydrophobic side chain to obtain a series of 2-*epi*-jaspine B analogs. The MTT assay was used to examine the antitumor activities of these analogs. We identified a novel 2-*epi*-jaspine B analog **YHR17**, which has potent antiproliferative activities for tested cell lines with IC_{50} values that ranged from 0.68 to 5.68 μM and inhibited the proliferation of the A375 cell line by affecting the cell cycle and apoptosis. Furthermore, **YHR17** inhibited SphK1 with more than 125-fold selectivity over SphK2.

Keywords: SphK1, SphK1 inhibitors, 2-*epi*-jaspine B, tetrahydropyrrolidine, anticancer.

1. Introduction

Sphingomyelin is one of the components of cell membranes, and its important metabolites ceramide (Cer), sphingosine (Sp) and sphingosine-1-phosphate (S1P) play important roles in regulating cell proliferation, migration and apoptosis. Cer and Sp can inhibit cell growth and promote apoptosis, whereas S1P promotes cell growth and inhibits apoptosis[1]. Sp can be phosphorylated to S1P by sphingosine kinases (SphKs), which are important rate-limiting enzymes that regulate the homeostasis of the above substances in cells[2]. There are two SphKs in mammals, SphK1[3] and SphK2[4]. SphK2 is mainly located in the cell nuclei. Recent studies have found that selective inhibition of the function of SphK2 can play a role in the treatment of various cancers such as liver cancer[5] and multiple myeloma[6]. However, the mechanisms for the physiological and pathological effects of SphK2 are still poorly understood. SphK1 is mainly located in the cytosol of eukaryotic cells, where it serves as a key kinase in the SphK1-S1P-S1P receptor (SphK1-S1P-S1PRs) signaling pathway (**Fig. 1**). By controlling the level of S1P, Cer and Sp in the cell, this enzyme regulates proliferation and apoptosis[7,8]. SphK1 is overexpressed in many tumor tissues[9,10] and is thus an ideal target for the treatment of cancers[11].

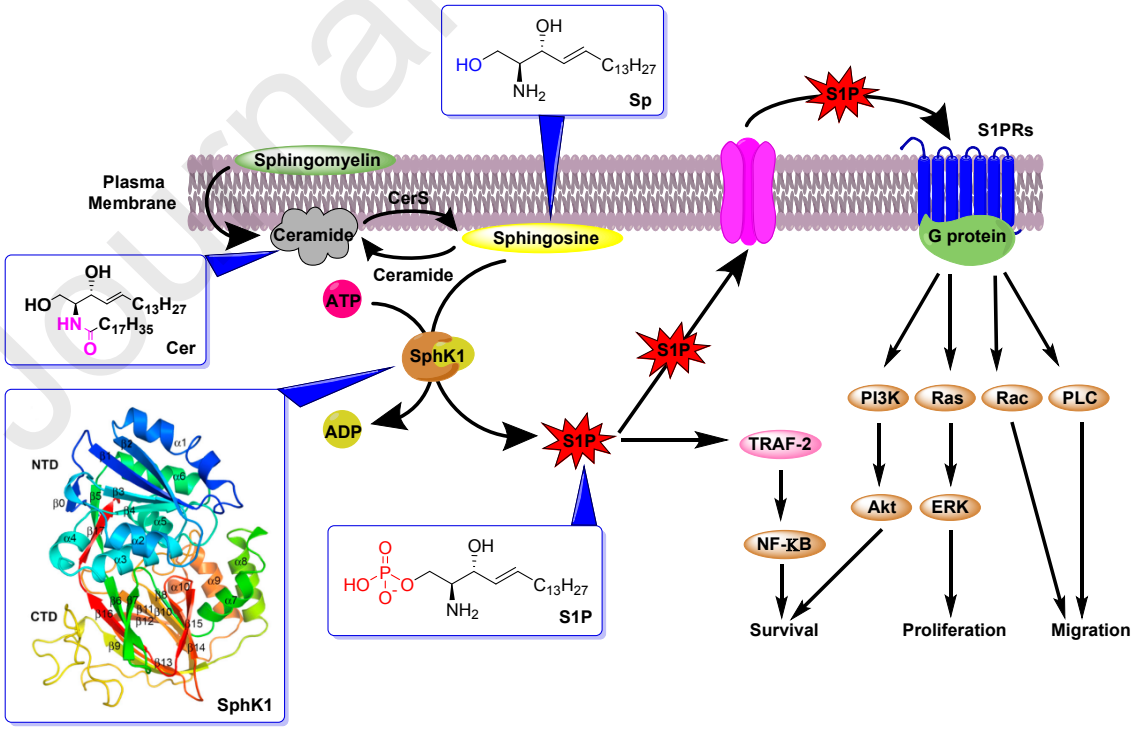

Fig. 1 SphK1-S1P-S1PRs signaling pathway

In the past few decades, various types of SphKs inhibitors have been developed[12] (**Fig. 2**). *N*,*N*-Dimethylsphingosine (DMS)[13] and SKI-II[14] can inhibit SphK1 and SphK2, protein kinase C and other kinases with low selectivity. PF-543 is a highly selective SphK1 inhibitor with 100-fold greater selectivity for SphK1 compared with SphK2; however, it cannot induce apoptosis in cancer cells[15,16]. Natural products are always an important source of drugs and lead compounds. The active natural product jaspine B (**Fig. 2**), which was isolated from the marine sponges *Jaspis* sp. in 2003[17], can be considered as an anhydrophytosphingosine derivative. Jaspine B contains an all-*cis*-2,3,4-trisubstituted tetrahydrofuran ring with the (2*S*,3*S*,4*S*) absolute configuration and exhibits potent antiproliferative activities against various human cancer cell lines by inhibiting SphKs[18-21]. Its 2-epimer has greater selectivity for SphK1[22] and demonstrates potent antiproliferative activities. Therefore, 2-*epi*-jaspine B can be used as an ideal precursor for the development of selective inhibitors of SphK1.

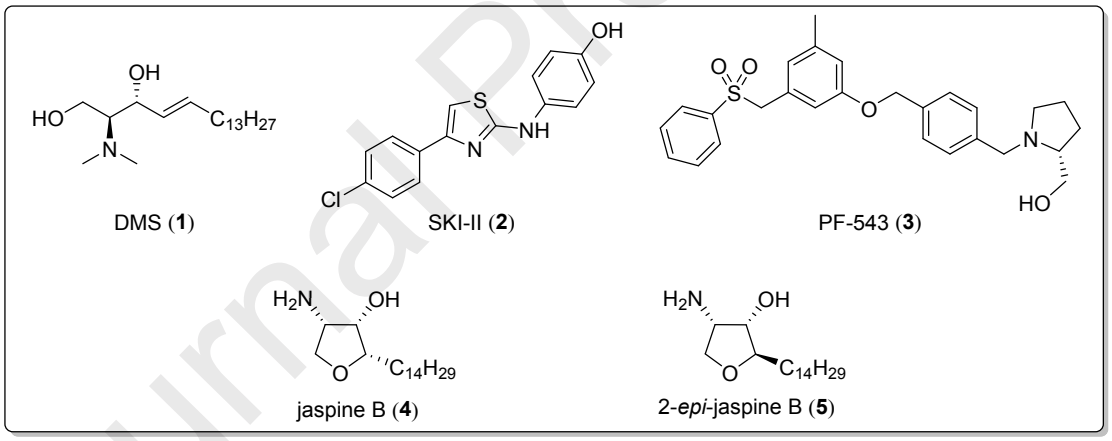

Fig. 2 Structures of SphKs inhibitors

Several synthetic[23-26] and structure–activity relationship (SAR) studies[27-29] have been conducted focused on jaspine B and 2-*epi*-jaspine B. Our group[30] has completed the total synthesis of tetrahydropyrrolidine analogs of 2-*epi*-jaspine B. Based on preliminary work, we continued to synthesize a series of novel 2-*epi*-jaspine B analogs, for which biological evaluation (including kinases and cells) and SAR analyses were also studied. These studies have contributed to the discovery of highly active and selective SphK1 inhibitors.

2. Results and discussion

2.1 Design and synthesis

The ligand-binding pocket of SphK1 is a "*J*-shaped" cavity. The head of the ligand-binding pocket of SphK1 is hydrophilic, wherein the corresponding amino acid residues can form hydrogen bonds with SphK1 inhibitors, and the endogenous substrate Sp can be phosphorylated to S1P. The tail portion of the binding pocket occupies a major portion of the active cavity and is a hydrophobic cavity that can accommodate a larger hydrophobic group or the center of an aromatic ring. SphK1 inhibitors regulate SphK1 function by interacting with the ligand-binding pocket of SphK1. Therefore, the design of an SphK1 inhibitor must be such that it cannot be phosphorylated and must fit appropriately into the ligand-binding pocket.

Given the analysis of the SphK1 binding pocket, as shown in **Fig. 3**, we retained the hydroxyl and amino groups on the tetrahydrofuran ring of 2-*epi*-jaspine B that acted as hydrogen bond donors/receptors and allowed them to form hydrogen bonds with the hydrophilic portion of the head of the binding pocket. Simultaneously, hydrophobic groups or aromatic ring centers of various sizes were introduced at the 2-position chiral side chain to match the tail hydrophobic cavity of the binding pocket, and the effects of the substituent groups on the biological activity of the analogs were investigated. In this context, we used the bioisosteric replacement to replace the tetrahydrofuran ring with a tetrahydropyrrole ring, which retained the rigid five-membered ring, and introduced an NH group that acted as a hydrogen bond donor/acceptor (forming a salt bridge with the amino acid residues) and enhanced the affinity of the compound for SphK1.

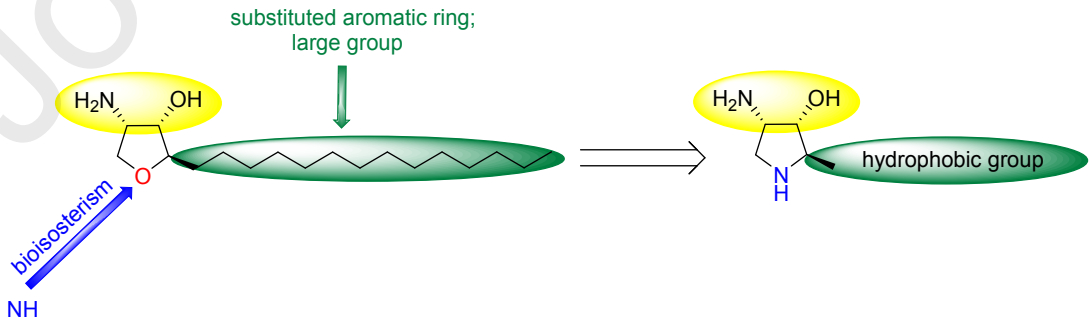

Fig. 3 Design of tetrahydropyrrolidine analogs

We synthesized a series of novel 2-*epi*-jaspine B analogs, **YHR1-YHR17,** based

on our previous studies, as well as the SAR studies of jaspine B and its 2-isomer, 2-*epi*-jaspine B. To obtain **YHR1-YHR17**, we first carried out the synthesis of terminal olefins shown in **Scheme 1**.

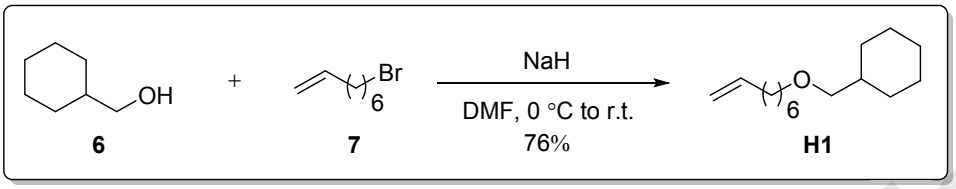

Scheme 1 Synthesis of **H1**

As shown in **Scheme 1**, the synthesis of terminal olefin **H1** (76% yield) was obtained by Williamson condensation of a known alcohol **6** with a halogenated olefin **7**. **H2-H14** were readily prepared in the same manner in 67%-82% yields, and the structures of the olefins are listed in **Table 1**.

Table 1 Structures of **H1-H14**

Code	Structure	Code	Structure
H1	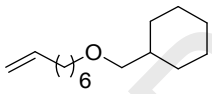	**H8**	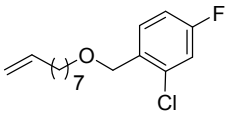
H2	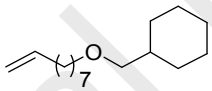	**H9**	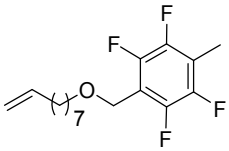
H3	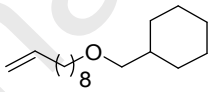	**H10**	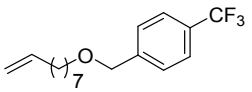
H4	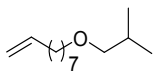	**H11**	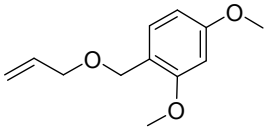
H5	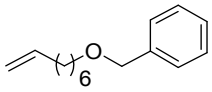	**H12**	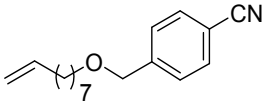
H6	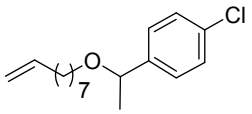	**H13**	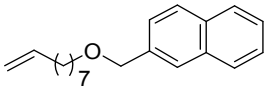
H7	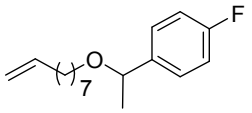	**H14**	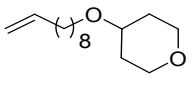

The pyrrolidine intermediates **8**[30] and **H14** were subjected to cross metathesis

reaction under the catalysis of the Grubbs^{2nd} catalyst, followed by hydrogenating the double bond and deprotecting the protecting groups on the amino and hydroxyl groups to give **YHR17** in 37% yield, as shown in **Scheme 2**. We used the same procedure as for **YHR17** to synthesize a series of 2-*epi*-jaspine B analogs, and their structures are listed in **Table 2**. All 2-*epi*-jaspine B analogs were characterized by ^{1}H NMR, ^{13}C NMR and HRMS spectra.

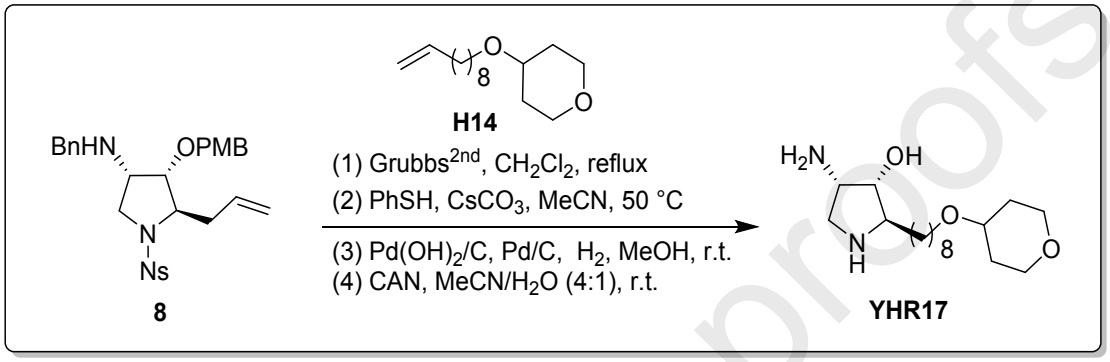

Scheme 2 Synthesis of **YHR17**

During the removal of the OPMB protecting group by CAN, there were two findings: 1) The CAN reagent eliminated the chlorine on the benzene ring, which resulted in the corresponding compounds **YHR9** and **YHR11**. 2) The CAN reagent removed the naphthylmethyl group (**H13**) of the ether group side chain on the hydrophobic group to form a hydroxyl group, which resulted in **YHR16**.

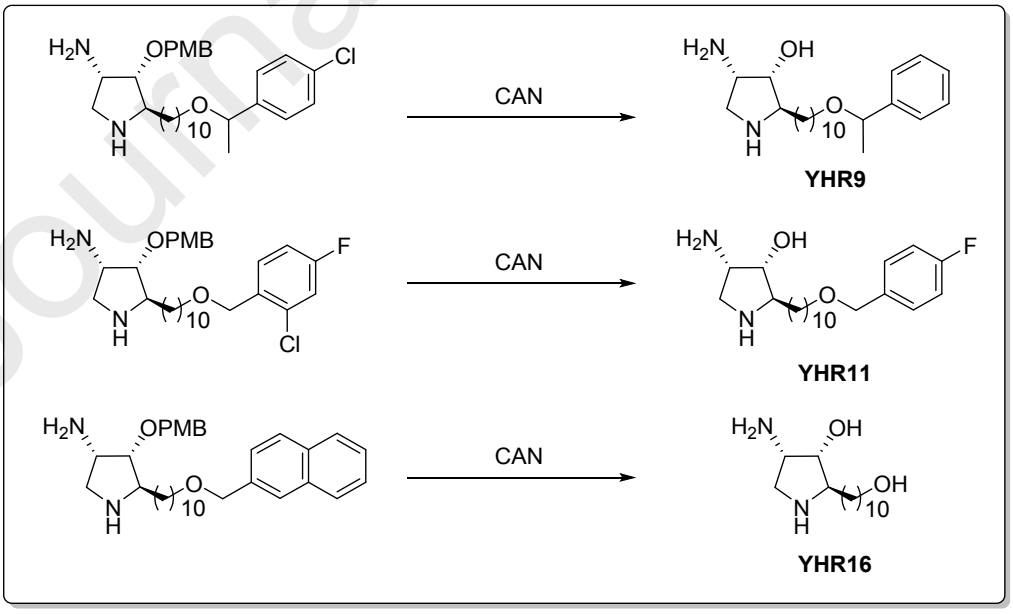

Scheme 3 CAN reagent eliminates chlorine and aromatic ring

Table 2 Structures of **YHR1-YHR17**

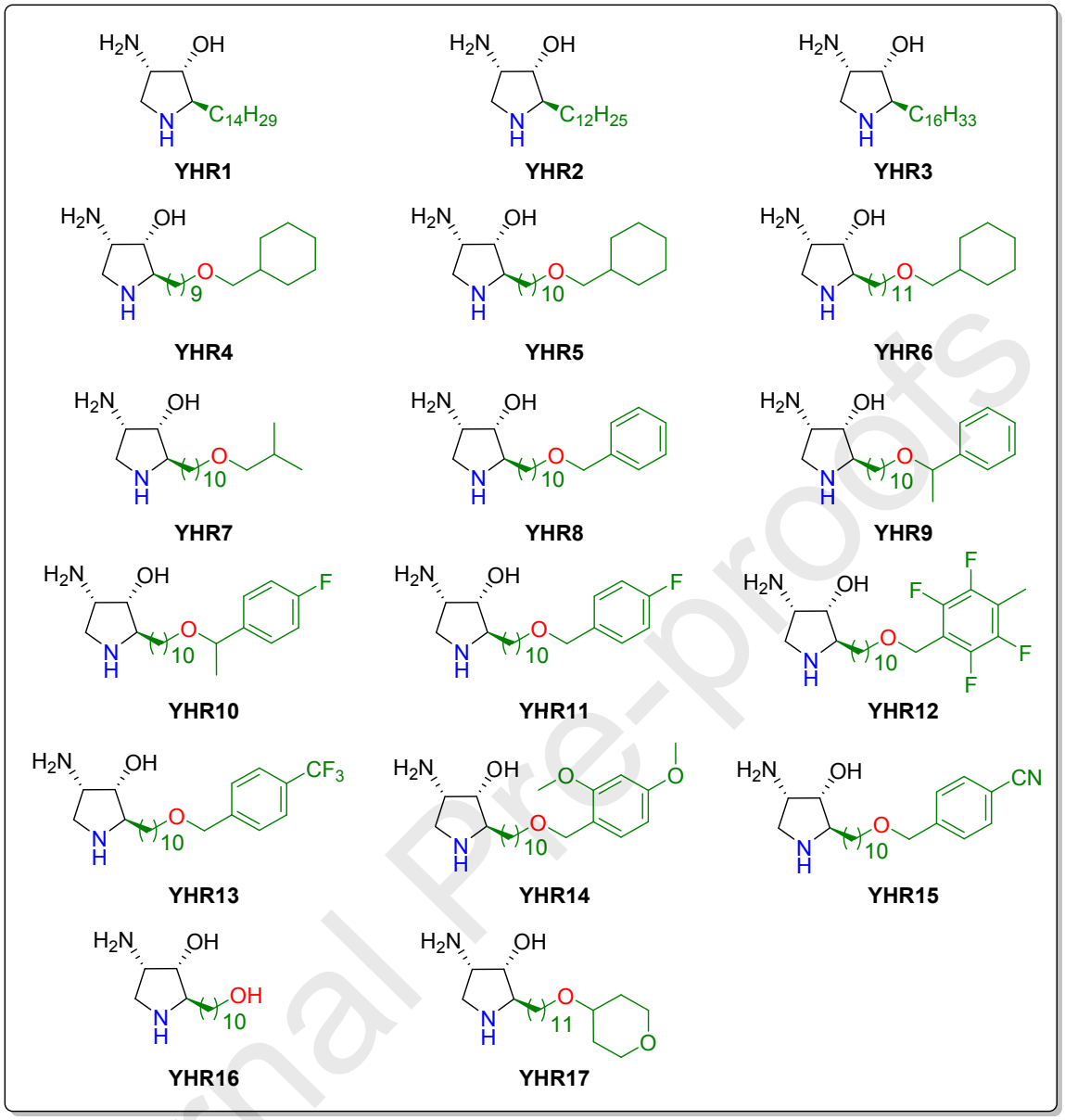

2.2 SAR studies

To carry out detailed structure-activity relationship (SAR) studies, all 2-*epi*-jaspine B analogs (**YHR1-YHR17**) were evaluated for antiproliferative activities on A549 and LOVO cell lines, and some of them were selected for preliminary tests for the inhibition of SphKs. The data for these biological evaluations are shown in **Table 3** and **Table 4**. Based on the data in **Table 3** and **Table 4**, we performed SAR analysis of the 2-*epi*-jaspine B analogs (**YHR1-YHR17**), and the results are summarized as follows.

Table 3 Antiproliferative activities of 2-*epi*- jaspine B and **YHR1-YHR17**

Compounds	IC_{50} (μM)[a]	
	A549	LOVO
2-*epi*-jaspine B	1.77±0.22	0.32±0.01
YHR1	0.02±0	0.05±0
YHR2	0.78±0.06	0.14±0.01
YHR3	3.02±0.18	4.42±0.29
YHR4	7.68±0.66	>10
YHR5	0.77±0.07	1.96±0.16
YHR6	0.36±0.02	0.18±0.01
YHR7	1.68±0.12	1.4±0.11
YHR8	1.81±0.16	0.66±0.05
YHR9	0.71±0.06	1.57±0.13
YHR10	2.88±0.23	2.06±0.19
YHR11	1.05±0.08	0.97±0.07
YHR12	0.67±0.04	0.58±0.05
YHR13	0.54±0.03	1.15±0.10
YHR14	9.55±1.80	>10
YHR15	0.73±0.06	0.19±0.01
YHR16	0.95±0.07	4.42±0.39
YHR17	5.68±0.55	0.68±0.05
Cisplatin[b]	0.49±0.05	0.72±0.06

[a]IC_{50} values were calculated from three independent experiments using the MTT assay after a 48 h treatment. The values are reported as the Means ± SD. [b]Cisplatin is a positive control anticancer drug. A549: Human non-small cell lung cancer cell line; LOVO: Human colon cancer cell line.

The results of **Table 3** and **Table 4** show that the antiproliferative activities of the modified tetrahydropyrrolidine analogs are close to or better than those of 2-*epi*-jaspine B. The replacement of the tetrahydrofuran ring in 2-*epi*-jaspine B by a tetrahydropyrrole

ring to obtain **YHR1** resulted in dramatic increases in the antiproliferative activities against a human non-small cell lung cancer cell line (A549) (IC_{50} = 20 nM) and a human colon cancer cell line (LOVO) (IC_{50} = 50 nM). However, as the carbon chain of the aliphatic chain increased or decreased, the antiproliferative activity decreased significantly, and the effect of an increase in the number of carbon atoms is particularly obvious (**YHR3**). To increase the matching degree of the compound to SphK1, we introduced a hydrophobic group or an aromatic ring of various sizes at the end of the long chain to investigate the effects of these substitutions on the selectivity and antiproliferative activity. The introduction of the terminal cyclohexane group (**YHR5** and **YHR6**) lead to a 3 or 4-fold increase in the antiproliferative activity compared with 2-*epi*-jaspine B. These effects on the activities were affected by the length of the carbon chain, and the activities increased as the carbon chain length increased. The replacement of the cyclohexane group in **YHR4** by a benzene (**YHR8**) and the cyclohexane group in **YHR5** by an isobutyl group (**YHR7**) lead to different results: the isobutyl group reduced the antiproliferative activity whereas benzene increased it. As shown in **Table 2**, the introduction of a large hydrophobic group increased the selectivity of the derivative for SphK1 compared to the long chain and 2-*epi*-jaspine B**,** which suggested that the large hydrophobic group was important for selectivity and antiproliferative activity. We next examined the effects of the α carbon on right side chain of the ether bond on antiproliferative activities by **YHR9-YHR11**. When the methyl group was introduced and there was an electron-withdrawing substituent on the benzene ring (**YHR10**), the antiproliferative activity was less than that of **YHR9,** which lacked these groups. Based on the results of this analysis, we concentrated on the favorable structural optimization on **YHR17**, hoping to increase the selectivity or improve the potency. To our surprise, as shown in **Table 3** and **Table 4,** the selectivity of **YHR17** for SphK1 over SphK2 was more than 125-fold, and this compound had potent antiproliferative activity against LOVO (IC_{50} = 0.68 μM). We introduced various electron-withdrawing and electron-donating substituents on the benzene to synthesize the analogs **YHR12-YHR15**. The results suggested that the electron-withdrawing substituents on the benzene ring could enhance the antiproliferative activity of the

analogs on the test cell lines whereas electron-donating substituents had the opposite effect. The unexpectedly obtained analog **YHR16** also exerted good antiproliferative activity, which indicated that the hydroxyl group of the long chain tail also played a certain role. Compared with 2-*epi*-jaspine B, **YHR17** had better selectivity, and the antiproliferative activity was also maintained. Thus, we selected two additional cancer cell lines to investigate the biological effects of **YHR17**.

Table 4 Comparison of 2-*epi*-jaspine B and its analogs on the inhibition of SphKs.

Compounds	IC_{50} (μM)[a]		Selectivity
	SphK1	SphK2	(SphK2/SphK1)
YHR3	13.8 ± 0.7	>100	>7.3
YHR4	9.7 ± 0.3	>100	>10.3
YHR5	4.9 ± 0.3	>100	>20.4
YHR7	6.9 ± 0.7	>100	>14.5
YHR17	0.8 ± 0.1	>100	>125
2-*epi*-jaspine B	4.3 ± 0.4	24.8 ± 2.8	5.8

[a]IC_{50} values were calculated from three independent experiments. The values were reported as the Means ± SD.

Next, we examined the antiproliferative activities of 2-*epi*-jaspine B and **YHR17** on a human malignant melanoma cell line (A375) and a human hepatoma cell line (HepG2). In addition, a normal human cardiac fibroblast cell line (HCFB) was also examined, with the aim of assessing the toxicity of **YHR17**. The results in **Table 5** shown that **YHR17** displayed potent antiproliferative activities on A375 (IC_{50} = 0.7 μM) and HepG2 (IC_{50} = 1.46 μM) cells. Furthermore, **YHR17** has no obvious cytotoxicity in the normal cell line HCFB (IC_{50} >100 μM).

Table 5 Comparison of 2-*epi*-jaspine B and **YHR17** on the growth of various cell lines.

compounds	IC_{50} (μM)[a]		
	A375	HepG2	HCFB
2-*epi*-jaspine B	0.53±0.01	2.12±0.15	>100

YHR17	0.70±0.09	1.46±0.12	>100
Cisplatin[b]	1.3±0.11	1.21±0.16	>100

[a]IC_{50} values are reported as the Means ± SD, which were derived from three independent experiments. [b]Cisplatin is a positive control anticancer drug. A375: Human malignant melanoma cell line; HepG2: Human hepatoma cell line; HCFB: Human cardiac fibroblast cell line.

2.3 YHR17 arrested the cell cycle at G1

The data in **Table 5** shown that **YHR17** has a significant antiproliferative activity on the A375 cell line. We therefore continued to study its biological effects in the A375 cell line. A propidium iodide (PI) staining kit was used to investigate the effect of **YHR17** on the cell cycle distribution. A375 cells were stained with PI and analyzed on a flow cytometer after treatment with **YHR17** (0.1 0.3, 1, 3 μM) and the control for 36 h.

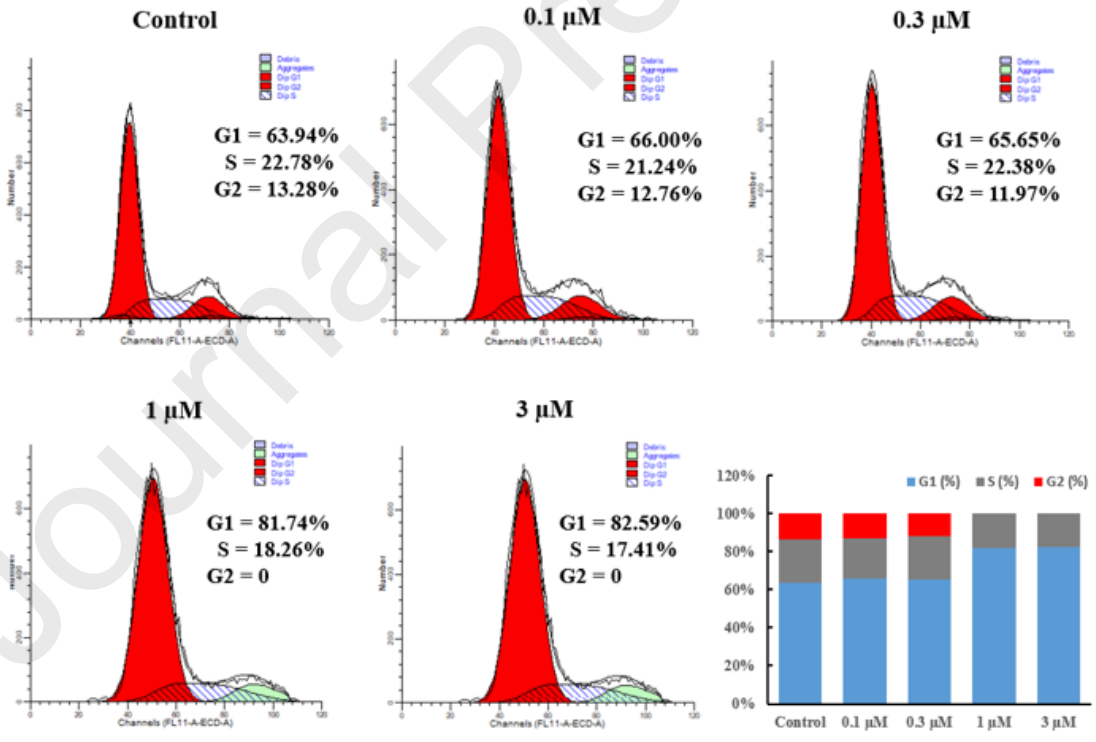

Fig. 4 YHR17 induced cell cycle arrest in A375 cells. The cells were treated with **YHR17** (0.1, 0.3, 1, 3 μM) for 36 h, fixed in cold 70% ethanol at -20 °C, and then stained with propidium iodide dye (10 μg/mL). The cell cycle analysis was evaluated using flow cytometry (FACSCalibur, Becton Dickinson, USA). The insert bar graph

showed the percentage (%) of the cells in the G1 and G2 phases.

Fig. 4 shows that as the concentration of **YHR17** increased, the cells in the G1 phase accumulated significantly compared to the control group (63.94%), with a range from 65.65% (0.1 μM) to 82.59% (3 μM), and exhibited concentration-dependence. Meanwhile, the cells in the G2 and S phases decreased from 13.28% to 0 and from 22.78% to 17.14%, respectively. From the above results, the mechanism of cytotoxicity of **YHR17** may be that it can arrest cell division at G1 phase.

2.4 YHR17 induced A375 cell apoptosis

A375 cells were examined using the Annexin V-FITC/PI FACS assay after being treated with **YHR17** (0.1, 0.3, 1, 3, 10, 33 μM) and Cisplatin (10 μM) for 48 h, with the aim of exploring the mechanism of cell death. **Fig. 5** shows that as the concentration of **YHR17** increased, the percentage of the apoptotic population in A375 cells increased significantly, with a range of 4.81% to 71.17% at 48 h. The apoptotic rate of A375 cells were positively correlated with the concentration of **YHR17** in a dose-dependent manner.

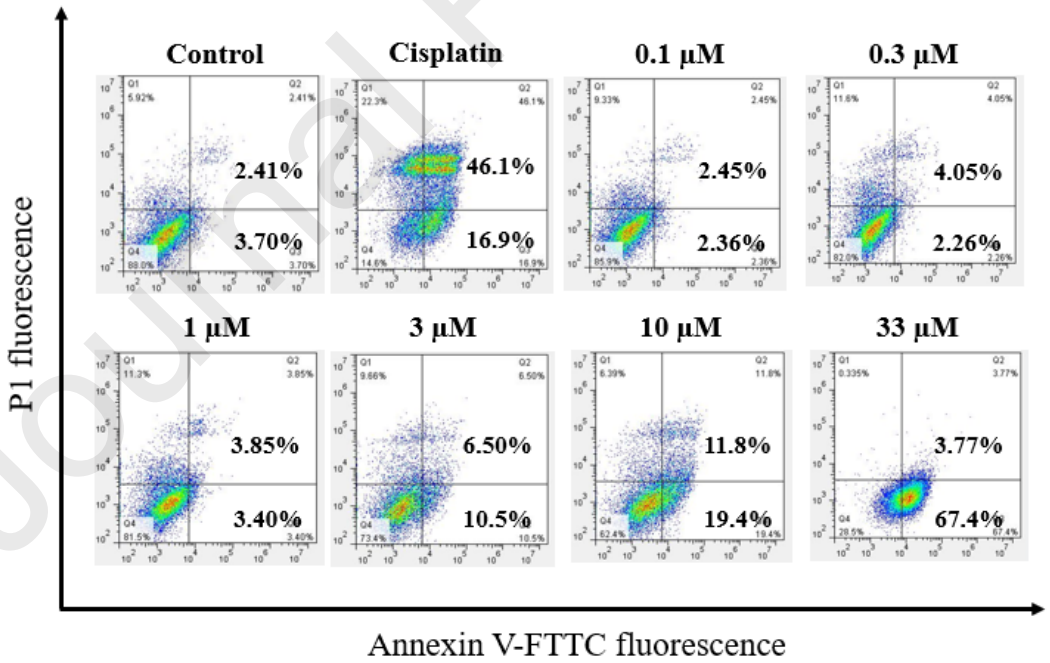

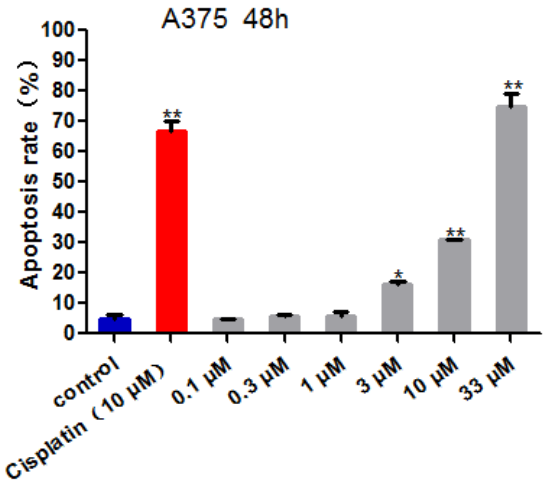

Fig. 5 YHR17 induced apoptosis in A375 cells. (A) A375 cells were treated for 48 h with various concentrations of **YHR17** as indicated. The cells were then stained with annexin V/PI, and apoptosis was analyzed using flow cytometry. The insert bar graph shows the statistics of total apoptotic cell percentages from duplicate experiments. **P < 0.05, *P < 0.01, versus the control group.

2.5 Docking mode analysis

To further investigate the reasons for the high selectivity of **YHR17** and support the SAR studies, we analyzed the molecular docking of **YHR17** with SphK1. The molecular docking analysis was performed using Discovery Studio 2019 based on the cocrystal structure of SphK1 and sphingosine (PDB ID: 3VZB).

As shown in **Fig. 6A**, the amino and hydroxyl groups on the tetrahydrofuran ring of 2-*epi*-jaspine B can form hydrogen bounds with the amino acid residues LEU268 and SER168 in the ligand-binding pocket of SphK1, and the long-chain aliphatic hydrocarbon of the 2-position can also contribute a certain hydrophobic effect. At the same time, it can be seen from the combination pattern that there is still a large space at the end of the 2-position, which could theoretically accommodate larger hydrophobic groups. As shown in **Fig. 6B,** the amino and hydroxyl groups on the ring of cationic form of **YHR17** can form hydrogen bonds with LEU268, SER168 and ASP81, and the NH_2^+ on the pyrrole ring can also serve as a hydrogen bond donor to ASP178 whereas the tetrahydrofuran ring of 2-*epi*-jaspine B has no such effect. In addition, a large group in the **YHR17** tail has a better hydrophobic effect than 2-*epi*-jaspine B. We then

performed a molecular docking analysis of the endogenous substrate sphingosine of SphK1 with **YHR17**. As shown in **Fig. 6C**, the spatial orientation of **YHR17** (thick gray line) is highly consistent with the substrate sphingosine (thin yellow line). From the above docking models, it can be concluded that the reasons for the relatively high inhibitory activity of YHR17 can be attributed to three points. 1) **YHR17** forms more hydrogen bounds with the ligand-binding pocket of SphK1. 2) The tetrahydropyran ring at the end of the side chain acts as a hydrophobic center that can interact hydrophobically with the corresponding amino acid residues. 3) The structure of **YHR17** is highly matched to the hydrophobic pocket of SphK1. The above analyses provide a reasonable explanation for the inhibitory activities and high selectivity of YHR17. Furthermore, the analyses provide a foundation for further studies, in which different hydrophobic groups as alkyl side chains may improve the isoform selectivity and inhibitory activity of these tetrahydropyrrolidine analogs.

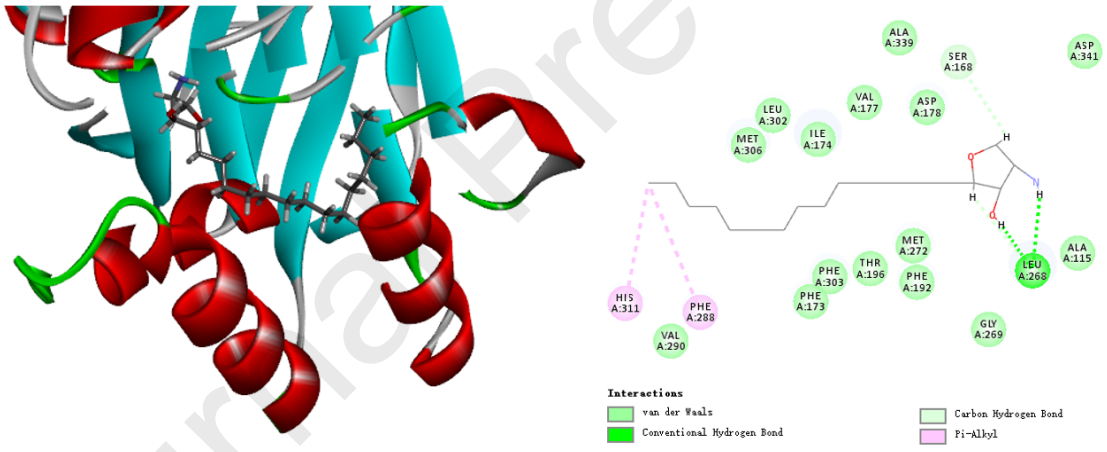

A

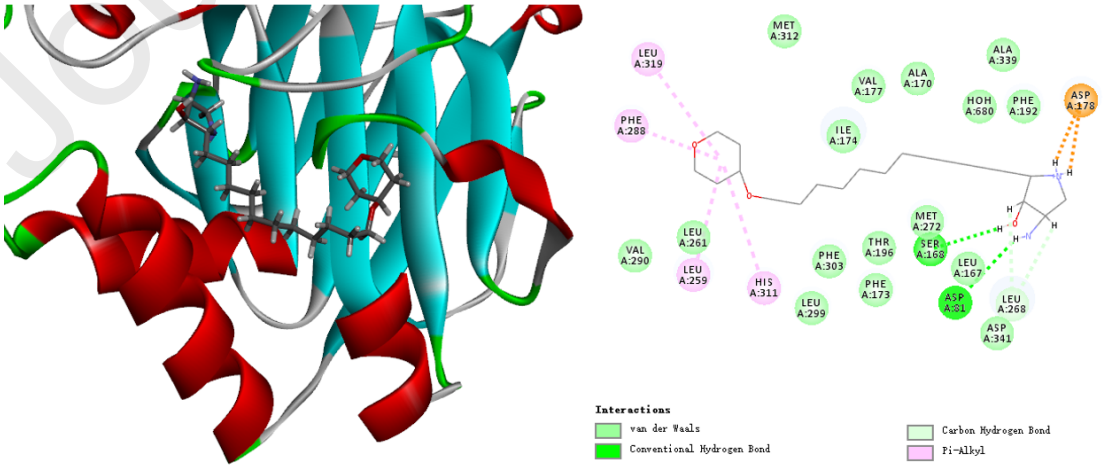

B

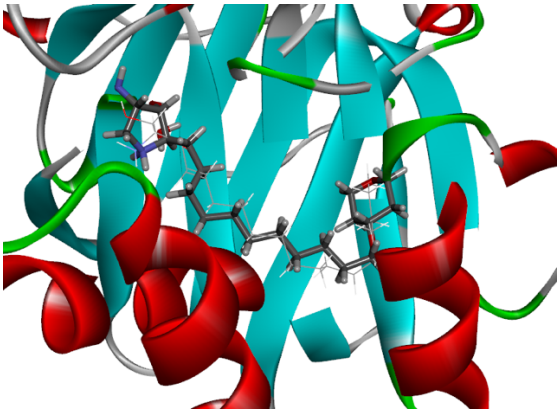

C

Fig. 6 (A) Electrostatic interactions between 2-*epi*-jaspine B and SphK1**.** Amino and hydroxyl groups are blue and red, respectively. **(B)** Predicted binding mode of **YHR17** and electrostatic interactions with SphK1**.** Amino and hydroxyl groups are blue and red, respectively. **(C)** Predicted binding mode of **YHR17** and sphingosine. The thick gray line represents **YHR17**, and the thin yellow line represents sphingosine.

3. Conclusion

In this study, we designed and synthesized some new analogs of 2-*epi*-jaspine B and tested their cytotoxic activities against A549, LOVO, A375, HepG2 cell lines and a normal cell line HCFB. In addition, we tested the inhibitory activities of these analogs against SphK1 and SphK2. Based on the results of the above experiments, we identified a novel 2-*epi*-jaspine B analog **YHR17**, which exhibited potent antiproliferative activities with IC_{50} values of 0.68 and 0.7 μM against LOVO and A375, respectively. Moreover, the IC_{50} value of **YHR17** against the normal cell line HCFB is more than 100 μM, thus demonstrating no obvious cytotoxicity. **YHR17** exhibited an anticancer activity comparable to that of 2-*epi*-jaspine B and exhibited inhibition of SphK1 with more than 125-fold selectivity over SphK2. Further biological evaluations suggested that **YHR17** arrested the cell cycle at the G1 phase and induced A375 cell apoptosis in a dose-dependent manner. We performed a systematic SAR analysis of 2-*epi*-jaspineB analogs and verified the results by molecular docking, based on the above data. All the results confirmed that **YHR17** is a potent and selective SphK1 inhibitor with good development prospects.

4. Experimental section

4.1 Materials and methods

All chemicals were purchased from commercial sources and used as received. For detailed information on the materials and methods, please see Supporting Information.

4.2 Synthesis of intermediates

All the synthetic procedures of intermediates are listed in Supporting Information.

4.3 Chemical synthesis and spectra data of the long-chain terminal olefins H1-H14

((oct-7-en-1-yloxy)methyl)cyclohexane (***H1***)

To a stirred solution of cyclohexylmethanol (**6**) (492 μL, 4.0 mmol, 2 eq) in DMF (7 mL) under argon was added NaH (60% suspension in mineral oil; 160 mg, 4.0 mmol, 2 eq) at 0 °C. The suspension was stirred at 0 °C for 30 min, then 8-bromodec-1-octene (**7**) (336 μL, 2.0 mmol, 1 eq) was added dropwise to the mixture. The mixture was allowed to warm to room temperature and stirred for 1 h. After the reaction was quenched with saturated NH_4Cl, the whole was extracted with Et_2O. The extract was washed with H_2O and brine, then dried over $MgSO_4$. The filtrate was concentrated under reduced pressure to give an oily residue, which was purified using silica gel chromatography (petroleum ether:EtOAc = 40:1) to afford **H1** (341 mg, 76% yield) as a colorless oil. ^{1}H NMR (CD_3OD, 600 MHz) δ (ppm): 5.81 (ddt, *J* = 16.9, 10.2, 6.7 Hz, 1H), 4.99 (dq, *J* = 17.1, 1.6 Hz, 1H), 4.93 (ddt, *J* = 10.2, 2.2, 1.2 Hz, 1H), 3.38 (t, *J* = 6.7 Hz, 2H), 3.19 (d, *J* = 6.6 Hz, 2H), 2.01–2.07 (m, 2H), 1.64–1.77 (m, 5H), 1.52–1.61 (m, 3H), 1.12–1.42 (m, 9H), 0.91 (dq, *J* = 12.3, 3.2 Hz, 2H). ^{13}C NMR ($CDCl_3$, 150 MHz) δ (ppm): 139.12, 114.16, 76.85, 71.09, 38.08, 33.76, 30.20 (2C), 29.71, 28.99, 28.89, 26.70, 26.07, 25.92 (2C). HRMS (ESI): calcd for $C_{15}H_{29}OH^+$ $[M+H]^+$ 225.2218, found 225.2220.

*((non-8-en-1-yloxy)methyl)cyclohexane (**H2**)*

Using a procedure with cyclohexylmethanol (**6**) (492 μL, 4.0 mmol, 2 eq) similar to that described for preparation of **H1**, 9-bromodec-1-nonene (371 μL, 2.0 mmol, 1 eq) was converted to **H2** (391 mg, 82% yield) as a colorless oil. ^{1}H NMR ($CDCl_3$, 600 MHz) δ (ppm): 5.80 (ddt, *J* = 17.0, 10.2, 6.7 Hz, 1H), 4.99 (dq, *J* = 17.1, 1.6 Hz, 1H), 4.92 (ddt, *J* = 10.2, 2.2, 1.2 Hz, 1H), 3.37 (t, *J* = 6.7 Hz, 2H), 3.19 (d, J = 6.6 Hz, 2H), 2.06

– 2.01 (m, 2H), 1.77–1.65 (m, 5H), 1.60–1.53 (m, 3H), 1.38–1.15 (m, 11H), 0.91 (qd, *J* = 12.3, 3.1 Hz, 2H). ^{13}C NMR ($CDCl_3$, 150 MHz) δ (ppm): 139.16, 114.12, 76.85, 71.11, 38.07, 33.79, 30.19 (2C), 29.74, 29.34, 29.09, 28.88, 26.69, 26.14, 25.91 (2C). HRMS (ESI): calcd for $C_{16}H_{30}OH^+$ $[M+H]^+$ 239.2375, found 239.2378.

*((dec-9-en-1-yloxy)methyl)cyclohexane (**H3**)*

Using a procedure with cyclohexylmethanol (**6**) (492 µL, 4.0 mmol, 2 eq) similar to that described for preparation of **H1**, 10-bromodec-1-decene (401 µL, 2.0 mmol, 1 eq) was converted to **H3** (414 mg, 82% yield) as a colorless oil. ^{1}H NMR ($CDCl_3$, 600 MHz) δ (ppm): 5.81 (ddt, *J* = 17.0, 10.2, 6.7 Hz, 1H), 4.99 (dq, *J* = 17.1, 1.6 Hz, 1H), 4.92 (ddt, *J* = 10.2, 2.4, 1.3 Hz, 1H), 3.37 (t, *J* = 6.7 Hz, 2H), 3.19 (d, *J* = 6.6 Hz, 2H), 2.01–2.06 (m, 2H), 1.64–1.77 (m, 5H), 1.51–1.61 (m, 3H), 1.15–1.37 (m, 13H), 0.91 (qd, *J* = 12.3, 3.1 Hz, 2H). ^{13}C NMR ($CDCl_3$, 150 MHz) δ (ppm): 139.20, 114.11, 76.86, 71.14, 38.08, 33.82, 30.20 (2C), 29.76, 29.46 (2C), 29.10, 28.94, 26.71, 26.19, 25.92 (2C). HRMS (ESI): calcd for $C_{17}H_{32}OH^+$ $[M+H]^+$ 253.2531, found 253.2517.

*9-isobutoxynon-1-ene (**H4**)*

Using a procedure with isobutyl alcohol (368 µL, 4.0 mmol, 2 eq) similar to that described for preparation of **H1**, 9-bromodec-1-nonene (371 µL, 2.0 mmol, 1 eq) was converted to **H4** (301 mg, 76% yield) as a colorless oil. ^{1}H NMR ($CDCl_3$, 400 MHz) δ (ppm): 5.81 (ddt, *J* = 16.9, 10.2, 6.7 Hz, 1H), 5.03-4.90 (m, 2H), 3.39 (t, *J* = 6.7 Hz, 2H), 3.16 (d, *J* = 6.7 Hz, 2H), 2.04 (q, *J* = 7.1 Hz, 2H), 1.80–1.90 (m, 1H), 1.53–1.60 (m, 2H), 1.25–1.42 (m, 8H), 0.90 (d, *J* = 6.7 Hz, 6H). ^{13}C NMR ($CDCl_3$, 100 MHz) δ (ppm): 139.19, 114.12, 77.85, 71.06, 33.79, 29.74, 29.34, 29.09, 28.88, 28.44, 26.15, 19.43 (2C). HRMS (ESI): calcd for $C_{13}H_{26}OH^+$ $[M+H]^+$ 199.2062, found 199.2056.

*((oct-7-en-1-yloxy)methyl)benzene (**H5**)*

Using a procedure with benzyl alcohol (416 µL, 4.0 mmol, 2 eq) similar to that described for preparation of **H1**, 9-bromodec-1-nonene (371 µL, 2.0 mmol, 1 eq) was converted to **H5** (323 mg, 74% yield) as a colorless oil. ^{1}H NMR ($CDCl_3$, 600 MHz) δ (ppm): 7.34 (d, *J* = 4.6 Hz, 4H), 7.27 (ddd, *J* = 8.8, 5.0, 3.9 Hz, 1H), 5.80 (ddt, *J* = 16.9, 10.2, 6.7 Hz, 1H), 4.99 (dq, *J* = 17.1, 1.6 Hz, 1H), 4.93 (ddt, *J* = 10.2, 2.3, 1.2 Hz, 1H), 4.50 (s, 2H), 3.46 (t, *J* = 6.6 Hz, 2H), 2.02–2.06 (m, 2H), 1.56–1.65 (m, 2H), 1.30–1.41

(m, 6H). ^{13}C NMR ($CDCl_3$, 150 MHz) δ (ppm): 139.13, 138.72, 128.35 (2C), 127.62 (2C), 127.47, 114.20, 72.88, 70.48, 33.75, 29.74, 28.97, 28.88, 26.08. HRMS (ESI): calcd for $C_{15}H_{22}ONa^+$ $[M+Na]^+$ 241.1568, found 241.1563.

*1-chloro-4-(1-(non-8-en-1-yloxy)ethyl)benzene (**H6**)*

Using a procedure with 1-(4-chlorophenyl) ethanol (541 μL, 4.0 mmol, 2 eq) similar to that described for preparation of **H1**, 9-bromodec-1-nonene (371 μL, 2.0 mmol, 1 eq) was converted to **H6** (410 mg, 73% yield) as a colorless oil. ^{1}H NMR ($CDCl_3$, 600 MHz) δ (ppm): 7.29–7.32 (m, 2H), 7.22–7.25 (m, 2H), 5.80 (ddt, *J* = 16.9, 10.2, 6.7 Hz, 1H), 4.99 (dq, *J* = 17.1, 1.6 Hz, 1H), 4.93 (ddt, *J* = 10.2, 2.2, 1.2 Hz, 1H), 4.35 (q, *J* = 6.5 Hz, 1H), 3.23–3.29 (m, 2H), 2.00–2.06 (m, 2H), 1.53–1.57 (m, 2H), 1.40 (d, *J* = 6.5 Hz, 3H), 1.34–1.38 (m, 2H), 1.24–1.31 (m, 6H). ^{13}C NMR (CD_3OD, 150 MHz) δ (ppm): 142.82,138.70, 132.67, 128.14 (2C), 127.41 (2C), 113.39, 77.18, 68.41, 33.49, 29.50, 28.94, 28.76, 28.67, 25.82, 22.97. HRMS (ESI): calcd for $C_{17}H_{25}ClOH^+$ $[M+H]^+$ 281.1672, found 281.1655.

*1-fluoro-4-(1-(non-8-en-1-yloxy)ethyl)benzene (**H7**)*

Using a procedure with 1-(4-fluorophenyl) ethanol (499 μL, 4.0 mmol, 2 eq) similar to that described for preparation of **H1**, 9-bromodec-1-nonene (371 μL, 2.0 mmol, 1 eq) was converted to **H7** (434 mg, 82% yield) as a colorless oil. ^{1}H NMR ($CDCl_3$, 600 MHz) δ (ppm): 7.27 (ddd, *J* = 8.3, 5.2, 2.8 Hz, 2H), 7.05- 6.99 (m, 2H), 5.80 (ddt, *J* = 16.9, 10.2, 6.7 Hz, 1H), 4.98 (dq, *J* = 17.1, 1.6 Hz, 1H), 4.92 (ddt, *J* = 10.2, 2.2, 1.2 Hz, 1H), 4.35 (q, *J* = 6.5 Hz, 1H), 3.22–3.29 (m, 2H), 2.00–2.06 (m, 2H), 1.52–1.57 (m, 2H), 1.40 (d, *J* = 6.5 Hz, 3H), 1.33–1.39 (m, 2H), 1.26–1.30 (m, 6H). ^{13}C NMR (CD_3OD, 150 MHz) δ (ppm): 162.14 (d, *J* = 241.5 Hz, 1C), 139.94, 138.69, 127.62, 127.57, 114.73, 114.58, 113.37, 77.18, 68.27, 33.48, 29.49, 28.94, 28.75, 28.67, 25.83, 23.04. HRMS (ESI): calcd for $C_{17}H_{25}FOH^+$ $[M+H]^+$ 265.1968, found 265.1952.

*2-chloro-4-fluoro-1-((non-8-en-1-yloxy)methyl)benzene (**H8**)*

Using a procedure with 2-chloro-4-fluorobenzyl alcohol (478 μL, 4.0 mmol, 2 eq) similar to that described for preparation of **H1**, 9-bromodec-1-nonene (371 μL, 2.0 mmol, 1 eq) was converted to **H8** (444 mg, 78% yield) as a colorless oil. ^{1}H NMR ($CDCl_3$, 600 MHz) δ (ppm): 7.45 (dd, *J* = 8.6, 6.2 Hz, 1H), 7.10 (dd, *J* = 8.5, 2.6 Hz,

1H), 6.98 (td, *J* = 8.4, 2.6 Hz, 1H), 5.81 (ddt, *J* = 16.9, 10.2, 6.7 Hz, 1H), 4.99 (dq, *J* = 17.1, 1.6 Hz, 1H), 4.93 (ddt, *J* = 10.2, 2.2, 1.2 Hz, 1H), 4.53 (s, 2H), 3.52 (t, *J* = 6.6 Hz, 2H), 2.01–2.07 (m, 2H), 1.60–1.67 (m, 2H), 1.35–1.41 (m, 4H), 1.31 (dt, *J* = 7.3, 3.4 Hz, 4H). ^{13}C NMR ($CDCl_3$,150 MHz) δ (ppm): 161.77 (d, *J* = 247.5Hz, 1C), 139.14, 133.42 (d, *J* = 10.5Hz, 1C), 132.40 (d, *J* = 4.5Hz, 1C), 130.04 (d, *J* = 4.5Hz, 1C), 116.58 (d, *J* = 24.0Hz, 1C), 114.18, 113.88 (d, *J* = 19.5Hz, 1C), 71.05, 69.26, 33.79, 29.71, 29.30, 29.07, 28.87, 26.14. HRMS (ESI): calcd for $C_{16}H_{22}ClFOH^+$ $[M+H]^+$ 285.1421, found 285.1420.

*1,2,4,5-tetrafluoro-3-methyl-6-((non-8-en-1-yloxy)methyl)benzene (**H9**)*

Using a procedure with 2,3,5,6-tetrafluoro-4-methylbenzyl alcohol (586 μL, 4.0 mmol, 2 eq) similar to that described for preparation of **H1**, 9-bromodec-1-nonene (371 μL, 2.0 mmol, 1 eq) was converted to **H9** (509 mg, 80% yield) as a colorless oil. ^{1}H NMR ($CDCl_3$, 600 MHz) δ (ppm): 5.80 (ddt, *J* = 16.9, 10.2, 6.7 Hz, 1H), 4.98 (dq, *J* = 17.1, 1.6 Hz, 1H), 4.92 (ddt, *J* = 10.2, 2.2, 1.2 Hz, 1H), 4.58 (s, 2H), 3.47 (t, *J* = 6.6 Hz, 2H), 2.27 (t, *J* = 2.1 Hz, 3H), 2.00–2.05 (m, 2H), 1.57 (p, *J* = 6.7 Hz, 2H), 1.31–1.39 (m, 4H), 1.26–1.30 (m, 4H). ^{13}C NMR ($CDCl_3$, 150 MHz) δ (ppm): 145.89 (ddd, *J* = 14.3, 6.7, 3.9 Hz, 1C), 145.63 (ddd, *J* = 14.4, 6.7, 4.0 Hz, 1C), 144.25 (ddd, *J* = 14.3, 6.7, 3.9 Hz, 1C), 144.01 (ddd, *J* = 14.4, 6.8, 3.9 Hz, 1C), 139.18, 116.29 (t, *J* = 19.1 Hz, 1C), 114.15, 113.66 (t, *J* = 18.0 Hz, 1C), 70.90, 59.78, 33.78, 29.56, 29.24, 29.05, 28.86, 25.98, 7.63. HRMS (ESI): calcd for $C_{17}H_{22}F_4OH^+$ $[M+H]^+$ 319.1685, found 319.1677.

*1-((non-8-en-1-yloxy)methyl)-4-(trifluoromethyl)benzene (**H10**)*

Using a procedure with 4-(trifluoromethyl) benzyl alcohol (548 μL, 4.0 mmol, 2 eq) similar to that described for preparation of **H1**, 9-bromodec-1-nonene (371 μL, 2.0 mmol, 1 eq) was converted to **H10** (457 mg, 76% yield) as a colorless oil. ^{1}H NMR ($CDCl_3$, 600 MHz) δ (ppm): 7.60 (d, *J* = 8.1 Hz, 2H), 7.45 (d, *J* = 8.1 Hz, 2H), 5.81 (ddt, *J* = 16.9, 10.2, 6.7 Hz, 1H), 4.99 (dq, *J* = 17.1, 1.6 Hz, 1H), 4.91–4.95 (m, 1H), 4.55 (s, 2H), 3.48 (t, *J* = 6.6 Hz, 2H), 2.04 (q, *J* = 7.0 Hz, 2H), 1.63 (dt, *J* = 14.6, 6.7 Hz, 2H), 1.37 (q, *J* = 11.7, 9.1 Hz, 4H), 1.31 (dq, *J* = 7.2, 4.4, 3.3 Hz, 4H). ^{13}C NMR ($CDCl_3$, 150 MHz) δ (ppm): 142.90, 139.15, 129.65 (q, *J* = 32.3 Hz, 1C), 127.48 (2C),

125.29 (q, *J* = 3.8 Hz, 2C), 123.32, 114.19, 72.06, 70.91, 33.79, 29.73, 29.32, 29.07, 28.87, 26.15. HRMS (ESI): calcd for $C_{17}H_{23}F_3OH^+$ $[M+H]^+$ 301.1779, found 301.1775.

*2,4-dimethoxy-1-((non-8-en-1-yloxy)methyl)benzene (**H11**)*

Using a procedure with 2,4-dimethoxybenzyl alcohol (606 μL, 4.0 mmol, 2 eq) similar to that described for preparation of **H1**, 9-bromodec-1-nonene (371 μL, 2.0 mmol, 1 eq) was converted to **H11** (456 mg, 78% yield) as a colorless oil. ^{1}H NMR ($CDCl_3$, 600 MHz) δ (ppm): 7.24 (d, *J* = 8.2 Hz, 1H), 6.43–6.49 (m, 2H), 5.80 (ddt, *J* = 17.0, 10.2, 6.7 Hz, 1H), 4.99 (dq, *J* = 17.1, 1.7 Hz, 1H), 4.92 (ddt, *J* = 10.2, 2.3, 1.2 Hz, 1H), 4.46 (s, 2H), 3.80 (d, *J* = 1.6 Hz, 6H), 3.46 (t, *J* = 6.7 Hz, 2H), 2.00–2.07 (m, 2H), 1.56–1.64 (m, 2H), 1.28–1.39 (m, 8H). ^{13}C NMR ($CDCl_3$,150 MHz) δ (ppm): 160.43, 158.39, 139.19, 130.10, 119.53, 114.12, 103.89, 98.42, 70.35, 67.30, 55.39, 55.35, 33.79, 29.76, 29.33, 29.10, 28.88, 26.16. HRMS (ESI): calcd for $C_{18}H_{28}O_3H^+$ $[M+H]^+$ 293.2117, found 293.2100.

*4-((non-8-en-1-yloxy)methyl)benzonitrile (**H12**)*

Using a procedure with 4-(hydroxymethyl) benzonitrile (459 μL, 4.0 mmol, 2 eq) similar to that described for preparation of **H1**, 9-bromodec-1-nonene (371 μL, 2.0 mmol, 1 eq) was converted to **H12** (422 mg, 82% yield) as a colorless oil. ^{1}H NMR ($CDCl_3$, 400 MHz) δ (ppm): 7.63 (d, *J* = 8.1 Hz, 2H), 7.44 (d, *J* = 8.0 Hz, 2H), 5.81 (ddt, *J* = 16.9, 10.2, 6.7 Hz, 1H), 4.96 (dd, *J* = 23.0, 13.7 Hz, 2H), 4.55 (s, 2H), 3.49 (t, *J* = 6.6 Hz, 2H), 2.04 (q, *J* = 7.1 Hz, 2H), 1.62 (td, *J* = 13.5, 6.7 Hz, 2H), 1.28–1.43 (m, 8H). ^{13}C NMR ($CDCl_3$, 100 MHz) δ (ppm): 144.39, 139.11, 132.19 (2C), 127.64 (2C), 118.91, 114.20, 111.16, 71.87, 71.12, 33.76, 29.69, 29.29, 29.04, 28.85, 26.12. HRMS (ESI): calcd for $C_{17}H_{23}NOH^+$ $[M+H]^+$ 258.1858, found 258.1860.

*2-((non-8-en-1-yloxy)methyl)naphthalene (**H13**)*

Using a procedure with 1-naphthalenemethanol (550 μL, 4.0 mmol, 2 eq) similar to that described for preparation of **H1**, 9-bromodec-1-nonene (371 μL, 2.0 mmol, 1 eq) was converted to **H13** (378 mg, 67% yield) as a colorless oil. ^{1}H NMR ($CDCl_3$, 600 MHz) δ (ppm): 8.11 (d, *J* = 8.3 Hz, 1H), 7.84 (d, *J* = 8.0 Hz, 1H), 7.78 (d, *J* = 8.2 Hz, 1H), 7.45–7.54 (m, 3H), 7.39–7.44 (m, 1H), 5.79 (ddt, *J* = 16.9, 10.2, 6.7 Hz, 1H), 4.98 (dd, *J* = 17.1, 1.9 Hz, 1H), 4.91–4.94 (m, 3H), 3.53 (t, *J* = 6.6 Hz, 2H), 2.01 (q, *J* = 7.0

Hz, 2H), 1.62 (dt, *J* = 14.5, 6.7 Hz, 2H), 1.30–1.40 (m, 4H), 1.27 (dt, *J* = 7.1, 3.4 Hz, 4H). ^{13}C NMR ($CDCl_3$, 150 MHz) δ (ppm): 139.15, 134.10, 133.74, 131.76, 128.46, 128.43, 126.22, 126.04, 125.68, 125.17, 124.07, 114.13, 71.41, 70.54, 33.77, 29.77, 29.26, 29.05, 28.84, 26.15. HRMS (ESI): calcd for $C_{20}H_{26}OH^+$ $[M+H]^+$ 283.2062, found 283.2072.

*4-(dec-9-en-1-yloxy)tetrahydro-2H-pyran (**H14**)*

Using a procedure with tetrahydro-4-pyranol (382 μL, 4.0 mmol, 2 eq) similar to that described for preparation of **H1**, 10-bromodec-1-decene (401 μL, 2.0 mmol, 1 eq) was converted to **H14** (346 mg, 72% yield) as a colorless oil. ^{1}H NMR ($CDCl_3$, 600 MHz) δ: 5.81 (ddt, *J* = 16.9, 10.2, 6.7 Hz, 1H), 4.99 (dq, *J* = 17.1, 1.6 Hz, 1H), 4.93 (ddt, *J* = 10.2, 2.2, 1.2 Hz, 1H), 3.94 (dt, *J* = 11.7, 4.3 Hz, 2H), 3.48–3.40 (m, 5H), 2.06–2.01 (m, 2H), 1.89 (ddt, *J* = 11.2, 5.2, 2.7 Hz, 2H), 1.61–1.54 (m, 4H), 1.41–1.27 (m, 10H).^{13}C NMR ($CDCl_3$, 150 MHz) δ: 139.20, 114.11,73.82, 67.78, 65.84 (2C), 33.79, 32.55 (2C), 30.07 29.43, 29.42, 29.07, 28.90, 26.21. HRMS (ESI): calcd for $C_{15}H_{28}O_2H^+$ $(M+H)^+$ 241.2168, found 241.2153.

4.4 Chemical synthesis and spectral data for the tetrahydropyrrolidine analogs YHR1-YHR17

(2R,3S,4S)-4-amino-2-(11-((tetrahydro-2H-pyran-4-yl)oxy)undecyl)pyrrolidin-3-ol (***YHR17***)

4-(dec-9-en-1-yloxy)tetrahydro-2H-pyran (**H14**) (179 mg, 0.744 mmol, 4 equiv) and Grubbs^{2nd} catalyst (31 mg, 0.037 mmol, 0.2 eq) were added to a solution of **8** (100 mg, 0.186 mmol, 1 eq) in anhydrous CH_2Cl_2 (6 mL) under a nitrogen atmosphere. After heating under reflux with stirring for 7 h, the resulting mixture was cooled to room temperature and filtered through a short silica gel column, which was eluted with EtOAc:CH_2Cl_2:hexane = 3 : 2 : 5. The solvent was removed under reduced pressure to give the crude metathesis product as a residue, which was dissolved in anhydrous MeCN (6 mL). $CsCO_3$ (52 mg, 0.372 mmol, 2 eq) and PhSH (28.7 μL, 0.28 mmol, 1.2 eq) were added to this mixture, and the resulting mixture was stirred at 50 ℃ under a hydrogen atmosphere for 3 h. The resulting mixture was cooled to room temperature and filtered through a short silica gel column, which was eluted with CH_2Cl_2. The

solvent was removed under reduced pressure to give the crude metathesis product as a residue, which was dissolved in anhydrous MeOH (6 mL). The solution was treated with 20% $Pd(OH)_2/C$ (30 mg) and 10% Pd/C (10 mg) at room temperature under a hydrogen atmosphere and stirred for 1d. The mixture was then filtered through a pad of celite and concentrated under reduced pressure to give the crude metathesis product as a residue, which was dissolved in a mixture of MeCN and water (4 : 1, 3.7 mL). Ammonium nitrate (467 mg, 1.78 mmol) was then added to this solution. After stirring at room temperature for 3 h, the mixture was then concentrated under reduced pressure to give an oily residue, which was purified by silica gel column chromatography (MeOH:EtOH:CH_2Cl_2:NH_4OH = 6:12:77:5) to afford **YHR17** (24 mg, 37% yield in 4 steps) as a white solid. $[\alpha]_D^{25}$ +13 (*c* = 0.1, MeOH), ^{1}H NMR (CD_3OD, 600 MHz) δ (ppm): 3.89 (dt, *J* = 11.5, 4.3 Hz, 2H), 3.58 (t, *J* = 5.4 Hz, 1H), 3.53–3.41 (m, 5H), 3.18–3.09 (m, 2H), 2.84 (q, *J* = 5.9 Hz, 1H), 2.55 (dd, *J* = 10.6, 7.2 Hz, 1H), 1.92–1.86 (m, 2H), 1.62–1.24 (m, 24H). ^{13}C NMR (CD_3OD,150 MHz) δ (ppm): 76.15, 73.63, 67.43, 65.31 (2C), 64.58, 53.54, 50.98, 33.90, 32.23 (2C), 29.72, 29.45, 29.34, 29.31 (2C), 29.29, 29.18, 26.68, 25.94.IR (KBr, cm^{-1}): 3350, 3244, 2922, 2661, 2536, 1641, 1585, 1469, 1361, 1166, 1136, 1114, 1087, 1006, 954, 893, 867, 821, 719, 626, 567. HRMS (ESI): calcd for $C_{14}H_{30}N_2O_2H^+$ $[M+H]^+$ 357.3117, found 357.3000.

(2R,3S,4S)-4-amino-2-tetradecylpyrrolidin-3-ol (***YHR1***)

With a four-step conversion using 1-tridecene similar to that described for preparation of **YHR17**, **8** was converted to **YHR1** (14 mg, 25% yield in 4 steps) as a white solid. $[\alpha]_D^{25}$ +10.4(*c* = 0.1, MeOH), ^{1}H NMR ($CDCl_3$, 400 MHz) δ (ppm): 3.48 (t, *J* = 5.6 Hz, 1H), 3.29–3.43 (m, 2H), 2.82 (q, *J* = 5.6 Hz, 1H), 2.60 (dq, *J* = 11.6, 6.0, 5.5 Hz, 1H), 1.84 (brs, 4H), 1.54–1.63 (m, 1H), 1.25 (s, 25H), 0.88 (t, *J* = 6.7 Hz, 3H). ^{13}C NMR ($CDCl_3$, 100 MHz) δ (ppm): 75.72, 65.00, 53.15, 51.73, 34.02, 31.85, 29.55, 29.58 (2C), 29.62 (4C), 29.48, 29.29, 26.75, 22.61,14.00. IR (KBr, cm^{-1}): 3348, 3242, 2918, 2850, 1558, 1469, 1458, 1377, 1350, 1118, 1080, 1028, 956, 908, 894, 869, 825, 719. HRMS (ESI): calcd for $C_{18}H_{38}N_2OH^+$ $[M+H]^+$ 299.3062, found 299.3047.

(2R,3S,4S)-4-amino-2-dodecylpyrrolidin-3-ol (***YHR2***)

With a four-step conversion using 1-undecene similar to that described for

preparation of **YHR17**, **8** was converted to **YHR2** (22 mg, 36% yield in 4 steps) as a white solid. $[\alpha]_D^{25}$ +13.3 (*c* = 0.12, MeOH), ^{1}H NMR (CD_3OD, 600 MHz) δ (ppm): 3.62–3.66 (m, 1H), 3.22 (q, *J* = 6.7 Hz, 1H), 3.17 (dd, *J* = 11.0, 6.7 Hz, 1H), 2.90 (q, *J* = 5.8 Hz, 1H), 2.62 (dd, *J* = 11.0, 7.4 Hz, 1H), 1.58–1.65 (m, 1H), 1.24–1.51 (m, 21H), 0.92 (t, *J* = 7.0 Hz, 3H). ^{13}C NMR (CD_3OD, 150 MHz) δ (ppm): 75.93, 64.58, 53.38, 50.68, 33.65, 31.69, 29.44, 29.42, 29.40, 29.38, 29.36, 39.30, 29.10, 26.66, 22.36, 13.07. IR (KBr, cm^{-1}): 3350, 3244, 2920, 2850, 2667, 2546, 1641, 1591, 1467, 1377, 1352, 1311, 1116, 1080, 1029, 954, 906, 871, 823, 719 cm^{-1}; HRMS (ESI): calcd for $C_{16}H_{34}N_2OH^+$ $[M+H]^+$ 271.2749, found 271.2629.

(2R,3S,4S)-4-amino-2-hexadecylpyrrolidin-3-ol (***YHR3***)

With a four-step conversion using 1-pentadecene similar to that described for preparation of **YHR17**, **8** was converted to **YHR3** (22 mg, 36% yield in 4 steps) as a white solid. $[\alpha]_D^{25}$ +12.1 (*c* = 0.12, MeOH), ^{1}H NMR (CD_3OD, 600 MHz) δ (ppm): 3.55–3.58 (m, 1H), 3.15 (q, *J* = 6.7 Hz, 1H), 3.09 (dd, *J* = 11.2, 6.7 Hz, 1H), 2.84 (q, *J* = 6.3 Hz, 1H), 2.56 (dd, *J* = 11.2, 7.5 Hz, 1H), 1.48–1.55 (m, 1H), 1.11–1.40 (m, 29H), 0.80 (t, *J* = 7.0 Hz, 3H). ^{13}C NMR ($CDCl_3$, 150 MHz) δ (ppm): 75.66, 65.09, 53.01, 51.91, 33.98, 31.90, 29.59, 29.63 (2C), 29.67 (6C), 29.52, 29.33, 26.79, 22.66, 14.07. IR (KBr, cm^{-1}): 3350, 3240, 2956, 2918, 2850, 1558, 1469, 1458, 1261, 1101, 1083, 1028, 954, 914, 883, 852, 804, 765, 719. HRMS (ESI): calcd for $C_{20}H_{42}N_2OH^+$ $[M+H]^+$ 327.3375, found 327.3231.

(2R,3S,4S)-4-amino-2-(9-(cyclohexylmethoxy)nonyl)pyrrolidin-3-ol (***YHR4***)

With a four-step conversion using **H1** similar to that described for preparation of **YHR17**, **8** was converted to **YHR4** (18 mg, 29% yield in 4 steps) as a colorless oil. $[\alpha]_D^{25}$ +15.3 (*c* = 0.1, MeOH), ^{1}H NMR ($CDCl_3$, 400 MHz) δ (ppm): 3.52 (t, *J* = 5.3 Hz, 1H), 3.36 (m, 4H), 3.19 (d, *J* = 6.6 Hz, 2H), 2.82–2.90 (m, 1H), 2.63 (dd, *J* = 9.7, 6.2 Hz, 1H), 2.41 (brs, 4H), 1.12–1.79 (m, 25H), 0.90 (q, *J* = 10.9, 10.1 Hz, 2H). ^{13}C NMR ($CDCl_3$, 100 MHz) δ (ppm): 76.83, 75.81, 71.13, 65.53, 53.29, 53.00, 38.04, 34.42, 30.18 (2C), 29.74 (2C), 29.55, 29.51, 29.48, 26.90, 26.69, 26.17, 25.90 (2C). IR (KBr, cm^{-1}): 3427 (br), 3248, 2924, 2850, 2792, 2665, 1463, 1448, 1409, 1375, 1122, 927, 910, 891, 844, 815, 723. HRMS (ESI): calcd for $C_{20}H_{40}N_2O_2H^+$ $[M+H]^+$ 341.3168,

found 341.3419.

(2R,3S,4S)-4-amino-2-(10-(cyclohexylmethoxy)decyl)pyrrolidin-3-ol (***YHR5***)

With a four-step conversion using **H2** similar to that described for preparation of **YHR17**, **8** was converted to **YHR5** (11 mg, 17% yield in 4 steps) as a colorless oil. $[\alpha]_D^{25}$ +9.4 (*c* = 0.06, MeOH), ^{1}H NMR (CD_3OD, 400 MHz) δ (ppm): 3.63 (t, *J* = 5.4 Hz, 1H), 3.39 (t, *J* = 6.5 Hz, 2H), 3.12–3.24 (m, 4H), 2.89 (q, *J* = 5.9 Hz, 1H), 2.61 (dd, *J* = 10.7, 7.2 Hz, 1H), 1.50–1.79 (m, 10H), 1.19–1.45 (m, 21H), 0.94 (q, *J* = 10.5, 9.0 Hz, 2H). ^{13}C NMR (CD_3OD, 100 MHz) δ (ppm): 76.48, 75.83, 70.75, 64.60, 53.31, 50.58, 37.93, 33.51, 29.83 (2C), 29.42, 29.34 (2C), 29.29, 29.27, 29.17, 26.64, 26.37, 26.89, 25.62 (2C). IR (KBr, cm^{-1}): 3338, 3253, 2924, 2850, 2792, 1558, 1541, 1454, 1373, 1124, 964, 916, 887, 815, 721. HRMS (ESI): calcd for $C_{21}H_{42}N_2O_2H^+$ $[M+H]^+$: 355.3325, found 355.3316.

(2R,3S,4S)-4-amino-2-(11-(cyclohexylmethoxy)undecyl)pyrrolidin-3-ol (***YHR6***)

With a four-step conversion using **H3** similar to that described for preparation of **YHR17**, **8** was converted to **YHR6** (16 mg, 23% yield in 4 steps) as a colorless oil. $[\alpha]_D^{25}$ +15.8 (*c* = 0.12, MeOH), ^{1}H NMR ($CDCl_3$, 400 MHz) δ (ppm): 3.52 (t, *J* = 5.3 Hz, 1H), 3.36 (m, 4H), 3.19 (d, *J* = 6.6 Hz, 2H), 2.86 (d, *J* = 5.2 Hz, 1H), 2.63 (dd, *J* = 9.6, 6.1 Hz, 1H), 2.31 (brs, 4H), 1.10–1.81 (m, 29H), 0.90 (q, *J* = 10.9, 10.1 Hz, 2H). ^{13}C NMR ($CDCl_3$, 100 MHz) δ (ppm): 76.83, 75.80, 71.15, 65.54, 53.26, 52.97, 38.05, 34.40, 30.18 (2C), 29.75 (2C), 29.59 (2C), 29.56, 29.55, 29.50, 26.91, 26.69, 26.18, 25.91 (2C). IR (KBr, cm^{-1}): 3348, 3244, 2922, 2850, 2792, 1558, 1541, 1465, 1448, 1406, 1375, 1124, 1014, 954, 889, 821, 721. HRMS (ESI): calcd for $C_{22}H_{44}N_2O_2H^+$ $[M+H]^+$ 369.3481, found 369.3477.

(2R,3S,4S)-4-amino-2-(10-isobutoxydecyl)pyrrolidin-3-ol (***YHR7***)

With a four-step conversion using **H4** similar to that described for preparation of **YHR17**, **8** was converted to **YHR7** (15 mg, 26% yield in 4 steps) as a colorless oil. $[\alpha]_D^{25}$ +7.8 (*c* = 0.06, MeOH), ^{1}H NMR (CD_3OD, 600 MHz) δ (ppm): 3.87 (t, *J* = 5.3 Hz, 1H), 3.52 (q, *J* = 6.6 Hz, 1H), 3.39 (dt, *J* = 18.7, 6.7 Hz, 3H), 3.20 (dd, *J* = 12.6, 6.9 Hz, 3H), 2.93 (dd, *J* = 11.8, 7.1 Hz, 1H), 1.77–1.89 (m, 1H), 1.69 (dt, *J* = 15.3, 7.8 Hz, 1H), 1.54 (dt, *J* = 14.4, 7.2 Hz, 3H), 1.16–1.49 (m, 18H), 0.90 (d, *J* = 6.7 Hz, 6H).

^{13}C NMR (CD_3OD, 150 MHz) δ (ppm): 77.51, 74.02, 70.07, 64.72, 51.99, 31.43, 29.36, 29.32, 29.23, 29.18, 29.15, 29.13, 28.19, 26.32, 25.91,18.37 (2C). IR (KBr, cm^{-1}): 3246, 3070, 2927, 2852, 1635, 1558, 1521, 1419, 1114, 1041, 1008, 968, 945, 873, 831, 819, 721. HRMS (ESI): calcd for $C_{18}H_{38}N_2O_2H^+$ $[M+H]^+$ 315.3012, found 315.3000.

(2R,3S,4S)-4-amino-2-(9-(benzyloxy)nonyl)pyrrolidin-3-ol (***YHR8***)

With a four-step conversion using **H5** similar to that described for preparation of **YHR17**, **8** was converted to **YHR8** (23 mg, 37% yield in 4 steps) as a white solid. $[\alpha]_D^{25}$ +14.8 (*c* = 0.11, MeOH), ^{1}H NMR ($CDCl_3$, 400 MHz) δ (ppm): 7.23–7.41 (m, 5H), 4.50 (s, 2H), 3.48 (dt, *J* = 21.9, 6.1 Hz, 3H), 3.29–3.37 (m, 2H), 2.85 (q, *J* = 5.8 Hz, 1H), 2.61 (dq, *J* = 11.7, 6.5, 5.7 Hz, 1H), 2.31 (brs, 4H), 1.06–1.68 (m, 16H). ^{13}C NMR ($CDCl_3$, 100 MHz) δ (ppm): 138.71, 128.33 (2C), 127.61 (2C), 127.45, 75.84, 72.85, 70.53, 66.51, 53.30, 53.06, 34.47, 29.77, 29.74, 29.53, 29.50, 29.46, 26.90, 26.18. IR (KBr, cm^{-1}): 3346, 3242, 2924, 2850, 2659, 2536, 1585, 1496, 1454, 1363, 1311, 1114, 1074, 1035, 964, 921, 910, 875, 825, 734, 698, 634, 609. HRMS (ESI): calcd for $C_{20}H_{34}N_2O_2H^+$ $[M+H]^+$ 335.2699, found 335.2696.

(2R,3S,4S)-4-amino-2-(10-(1-phenylethoxy)decyl)pyrrolidin-3-ol (***YHR9***)

With a four-step conversion using **H6** similar to that described for preparation of **YHR17**, **8** was converted to **YHR9** (23 mg, 34% yield in 4 steps) as a colorless oil. $[\alpha]_D^{25}$ +16.2 (*c* = 0.12, MeOH), ^{1}H NMR (CD_3OD, 400 MHz) δ (ppm): 7.23–7.34 (m, 5H), 4.40 (q, *J* = 6.5 Hz, 1H), 3.63 (t, *J* = 5.3 Hz, 1H), 3.30 (dt, *J* = 13.4, 7.6 Hz, 3H), 3.18 (ddd, *J* = 17.6, 11.9, 6.6 Hz, 2H), 2.89 (q, *J* = 5.8 Hz, 1H), 2.60 (dd, *J* = 10.6, 7.1 Hz, 1H), 1.08–1.66 (m, 24H). ^{13}C NMR (CD_3OD, 100 MHz) δ (ppm): 143.88, 128.07 (2C), 127.10, 125.82 (2C), 77.94, 75.91, 68.37, 64.59, 53.38, 50.72, 33.68, 29.55, 29.45, 29.32, 29.30, 29.29, 29.15, 26.66, 25.90, 23.15. IR (KBr, cm^{-1}): 3344, 3267, 3028, 2926, 2852, 1647, 1558, 1541, 1456, 1406, 1369, 1280, 1207, 1105, 815, 759, 700, 611, 559. HRMS (ESI): calcd for $C_{22}H_{38}N_2O_2H^+$ $[M+H]^+$ 363.3012, found 363.2998.

(2R,3S,4S)-4-amino-2-(10-(1-(4-fluorophenyl)ethoxy)decyl)pyrrolidin-3-ol (***YHR10***)

With a four-step conversion using **H7** similar to that described for preparation of **YHR17**, **8** was converted to **YHR10** (27 mg, 38% yield in 4 steps) as a colorless oil.

$[\alpha]_D^{25}$ +13.7 (*c* = 0.12, MeOH), ^{1}H NMR ($CDCl_3$, 400 MHz) δ (ppm): 7.27 (t, *J* = 6.7 Hz, 2H), 7.02 (t, *J* = 8.6 Hz, 2H), 4.36 (q, *J* = 6.3 Hz, 1H), 3.52 (t, *J* = 4.8 Hz, 1H), 3.35 (dq, *J* = 16.2, 6.7 Hz, 2H), 3.25 (q, *J* = 9.0, 7.6 Hz, 2H), 2.80–2.89 (m, 1H), 2.56–2.69 (m, 1H), 1.03–1.71 (m, 25H). ^{13}C NMR ($CDCl_3$, 100 MHz) δ (ppm): 162.03 (d, *J* = 243.0Hz), 140.03, 127.65 (d, *J* = 7.0Hz, 2C), 115.14 (d, *J* = 21.0Hz, 2C), 77.18, 75.81, 68.73, 65.53, 53.29, 53.01, 34.44, 29.91, 29.75, 29.55, 29.54 (2C), 29.43, 26.90, 26.17, 24.20. IR (KBr, cm^{-1}): 3400 (br), 3253, 2926, 2854, 1645, 1606, 1560, 1510, 1456, 1369, 1340, 1224, 1103, 1016, 887, 837, 725, 640, 580. HRMS (ESI): calcd for $C_{22}H_{37}FN_2O_2H^+$ $[M+H]^+$ 381.2917, found 381.2761.

(2R,3S,4S)-4-amino-2-(10-((4-fluorobenzyl)oxy)decyl)pyrrolidin-3-ol (***YHR11***)

With a four-step conversion using **H8** similar to that described for preparation of **YHR17**, **8** was converted to **YHR11** (18 mg, 26% yield in 4 steps) as a colorless oil. $[\alpha]_D^{25}$ +14.3 (*c* = 0.11, MeOH), ^{1}H NMR (CD_3OD, 400 MHz) δ (ppm): 7.29–7.38 (m, 2H), 7.05 (t, *J* = 8.7 Hz, 2H), 4.46 (s, 2H), 3.63 (t, *J* = 5.3 Hz, 1H), 3.47 (t, *J* = 6.5 Hz, 2H), 3.18 (ddd, *J* = 17.5, 12.0, 6.7 Hz, 2H), 2.89 (q, *J* = 5.8 Hz, 1H), 2.61 (dd, *J* = 10.7, 7.2 Hz, 1H), 1.20–1.67 (m, 22H). ^{13}C NMR (CD_3OD, 100 MHz) δ (ppm): 162.32 (d, *J* = 242.0Hz), 134.50, 129.35 (d, *J* = 8.0Hz, 2C), 114.63 (d, *J* = 21.0Hz, 2C), 75.85, 71.71, 70.08, 64.60, 53.33, 50.62, 33.58, 29.41, 29.35, 29.31, 29.27, 29.26, 29.14, 26.63, 25.88. IR (KBr, cm^{-1}): 3348, 3242, 2922, 2850, 2791, 2659, 2528, 1514, 1465, 1363, 1298, 1240, 1120, 1016, 966, 921, 879, 821, 767, 721, 634, 567. HRMS (ESI): calcd for $C_{21}H_{35}FN_2O_2H^+$ $[M+H]^+$ 367.2761, found 367.2761.

(2R,3S,4S)-4-amino-2-(10-((2,3,5,6-tetrafluoro-4-methylbenzyl)oxy)decyl)pyrrolidin-3-ol (***YHR12***)

With a four-step conversion using **H9** similar to that described for preparation of **YHR17**, **8** was converted to **YHR12** (27 mg, 33% yield in 4 steps) as a white solid. $[\alpha]_D^{25}$ +12.1 (*c* = 0.13, MeOH), ^{1}H NMR (CD_3OD, 600 MHz) δ (ppm): 4.59 (s, 2H), 3.67 (t, *J* = 5.4 Hz, 1H), 3.49 (t, *J* = 6.5 Hz, 2H), 3.26 (q, *J* = 6.7 Hz, 1H), 3.19 (dd, *J* = 11.2, 6.7 Hz, 1H), 2.91–2.97 (m, 1H), 2.66 (dd, *J* = 11.3, 7.5 Hz, 1H), 2.28 (s, 3H), 1.59 (ddt, *J* = 27.5, 14.0, 7.6 Hz, 3H), 1.22–1.49 (m, 19H). ^{13}C NMR ($CDCl_3$, 100 MHz) δ (ppm): 146.20, 145.92, 143.86, 143.56, 116.25 (t, *J* = 19.0Hz, 1C), 113.64 (t, *J* = 18.0Hz,

1C), 75.81, 70.90, 65.54, 59.74, 53.31, 52.99, 34.43, 29.74, 29.55, 29.52 (3C), 29.37, 26.89, 25.99, 7.61. IR (KBr, cm^{-1}): 3350, 3244, 2920, 2850, 2686, 2538, 1633, 1581, 1487, 1409, 1367, 1284, 1109, 1072, 1031, 956, 923, 875, 837, 752, 719, 667, 597. HRMS (ESI): calcd for $C_{22}H_{34}F_4N_2O_2H^+$ $[M+H]^+$ 435.2635, found 435.2453.

(2R,3S,4S)-4-amino-2-(10-((4-(trifluoromethyl)benzyl)oxy)decyl)pyrrolidin-3-ol (***YHR13***)

With a four-step conversion using **H10** similar to that described for preparation of **YHR17**, **8** was converted to **YHR13** (27 mg, 35% yield in 4 steps) as a white solid. $[\alpha]_D^{25}$ +16.1 (*c* = 0.0.13, MeOH), ^{1}H NMR ($CDCl_3$, 400 MHz) δ (ppm): 7.60 (d, *J* = 8.0 Hz, 2H), 7.45 (d, *J* = 7.9 Hz, 2H), 4.55 (s, 2H), 3.50 (dt, *J* = 19.5, 6.0 Hz, 3H), 3.30–3.43 (m, 2H), 2.87 (d, *J* = 5.3 Hz, 1H), 2.64 (dd, *J* = 9.7, 6.1 Hz, 1H), 2.40 (brs, 4H), 1.11–1.68 (m, 18H). ^{13}C NMR ($CDCl_3$, 100 MHz) δ (ppm): 142.90, 129.60 (d, *J* = 32.0Hz), 127.46 (2C), 125.26 (q, *J* = 3.8Hz, 2C), 122.85, 75.76, 72.02, 70.93, 65.52, 53.14, 52.94, 34.33, 29.73 (2C), 29.56, 29.54 (2C), 29.46, 26.89, 26.17. IR (KBr, cm^{-1}): 3350, 3240, 2926, 2850, 1622, 1558, 1469, 1406, 1340, 1165, 1124, 1066, 1018, 970, 921, 879, 823, 758, 646, 594. HRMS (ESI): calcd for $C_{22}H_{35}F_3N_2O_2H^+$ $[M+H]^+$: 417.2729, found 417.2721.

(2R,3S,4S)-4-amino-2-(10-((2,4-dimethoxybenzyl)oxy)decyl)pyrrolidin-3-ol (***YHR14***)

With a four-step conversion using **H11** similar to that described for preparation of **YHR17**, **8** was converted to **YHR14** (14 mg, 19% yield in 4 steps) as a white solid. $[\alpha]_D^{25}$ +15.7 (*c* = 0.09, MeOH), ^{1}H NMR (CD_3OD, 600 MHz) δ (ppm): 7.09 (d, *J* = 8.3 Hz, 1H), 6.42 (d, *J* = 2.3 Hz, 1H), 6.38 (dd, *J* = 8.3, 2.3 Hz, 1H), 4.33 (s, 2H), 3.70 (s, 3H), 3.69 (s, 3H), 3.54–3.57 (m, 1H), 3.36 (t, *J* = 6.6 Hz, 2H), 3.14 (q, *J* = 6.7 Hz, 1H), 3.08 (dd, *J* = 11.2, 6.7 Hz, 1H), 2.82 (q, *J* = 6.1 Hz, 1H), 2.54 (dd, *J* = 11.2, 7.5 Hz, 1H), 1.44–1.54 (m, 3H), 1.15–1.40 (m, 19H). ^{13}C NMR (CD_3OD, 150 MHz) δ (ppm): 161.01, 158.72, 130.32, 118.56, 103.89, 97.80, 75.63, 69.79, 67.08, 64.62, 54.46, 54.37, 53.16, 50.31, 33.30, 29.36, 29.31, 29.27, 29.25, 29.23, 29.11, 26.58, 25.82. IR (KBr, cm^{-1}): 3433 (br), 3269, 2926, 2850, 1618, 1510, 1259, 1209, 1138, 1093, 970, 920, 869, 829, 790, 719, 634, 565. HRMS (ESI): calcd for $C_{23}H_{40}N_2O_4H^+$ $[M+H]^+$ 409.3066, found 409.2900.

4-(((10-((2R,3S,4S)-4-amino-3-hydroxypyrrolidin-2-yl)decyl)oxy)methyl)benzonitrile (***YHR15***)

With a four-step conversion using **H12** similar to that described for preparation of **YHR17**, **8** was converted to **YHR15** (18 mg, 26% yield in 4 steps) as a white solid. $[\alpha]_D^{25}$ +15.5 (*c* = 0.11, MeOH), ^{1}H NMR (CD_3OD, 600 MHz) δ (ppm): 7.22 (d, *J* = 8.0 Hz, 2H), 7.16 (d, *J* = 7.9 Hz, 2H), 4.45 (s, 2H), 3.64 (dd, *J* = 6.0, 4.9 Hz, 1H), 3.47 (t, *J* = 6.6 Hz, 2H), 3.14–3.24 (m, 2H), 2.90 (dt, *J* = 7.2, 5.5 Hz, 1H), 2.62 (dd, *J* = 11.0, 7.4 Hz, 1H), 1.56–1.64 (m, 3H), 1.26–1.51 (m, 15H). ^{13}C NMR (CD_3OD, 150 MHz) δ (ppm): 137.03, 135.34, 128.56 (2C), 127.59 (2C), 75.89, 72.34, 69.87, 64.59, 50.65, 33.61, 29.41, 29.33, 29.31, 29.27, 29.25, 29.13, 26.63, 25.86, 19.83. IR (KBr, cm^{-1}): 3348, 3242, 2920, 2850, 2657, 2520, 1720, 1587, 1516, 1465, 1367, 1114, 1020, 960, 920, 877, 833, 800, 754, 719, 682, 655, 632, 567. HRMS (ESI): calcd for $C_{22}H_{35}N_3O_2Na^+$ $[M+Na]^+$ 396.6080, found 396.6080.

(2R,3S,4S)-4-amino-2-(10-hydroxydecyl)pyrrolidin-3-ol (***YHR16***)

With a four-step conversion using **H13** similar to that described for preparation of **YHR17**, **8** was converted to **YHR16** (13 mg, 28% yield in 4 steps) as a white solid. $[\alpha]_D^{25}$ +20.3 (*c* = 0.12, MeOH), ^{1}H NMR ($CDCl_3$, 400 MHz) δ (ppm): 3.59 (t, *J* = 6.6 Hz, 3H), 3.20–3.31 (m, 2H), 3.12 (brs, 5H), 2.90 (q, *J* = 6.6, 5.9 Hz, 1H), 2.62 (dd, *J* = 10.1, 6.7 Hz, 1H), 1.08–1.65 (m, 18H). ^{13}C NMR ($CDCl_3$, 100 MHz) δ (ppm): 75.74, 65.00, 62.49, 53.18, 51.84, 34.03, 32.52, 29.50, 29.38, 29.31, 29.29, 29.26, 26.66, 25.63. IR (KBr, cm^{-1}): 3342, 3248, 2922, 2850, 2659, 2528, 1649, 1558, 1467, 1431, 1354, 1321, 1109, 1062, 1020, 966, 920, 877, 831, 786, 719, 634, 570, 513. HRMS (ESI): calcd for $C_{14}H_{30}N_2O_2H^+$ $[M+H]^+$ 259.2386, found 259.2380.

4.5 Cell viability

The viability of four cancer cell lines and one normal cardiac fibroblast cell line was assessed using the MTT assay after the treatment of **YHR1-YHR17**, and 2-*epi*-jaspine B. **YHR1-YHR17** and 2-*epi*-jaspine B were dissolved in pure DMSO to a concentration of 10 mM and diluted with the culture medium during the experiment. Five cell lines (A549, LOVO, A375, HepG2, and HCFB) were plated at a density of 6×10^3 per well in 96-well plates. After culturing for 24 h, **YHR1-YHR17** and 2-*epi*-

jaspine B (0.01, 0.1, 1, 10 and 100 μM), Cisplatin, or DMSO (4%) was added and incubated for 48 h at 37 °C. Then, 10 μL of a solution of MTT (5 mg/mL in PBS) was added to each well in the 96-well plates, and the cells were cultured for another 4 h. After the medium was removed, 150 μL DMSO was added. The OD value of each well was measured at 570 nm in a microplate reader (Bio-Rad Laboratories). Finally, the IC_{50} values were calculated, and the mean values from three independent experiments were calculated.

4.6 Cell cycle

The A375 cells were seeded at 1×10^6 well^{-1} in six-well plates and treated with **YHR17** (0.1, 0.3, 1, 3 μM) and control for 36 h at 37 °C. The medium was then removed, and the cells were washed three times with cold PBS. Then, the cells were harvested and fixed overnight at -20 °C with 70% ethanol precooled to -20 °C. The A375 cells were then treated with RNase A and stained with PI. Finally, the suspended cells were analyzed using a flow cytometer (FACSCalibur, BD Biosciences).

4.7 Cell apoptosis

The A375 cells were seeded at 1×10^6 well^{-1} on each well of six-well plates and incubated for 48 h. Then, the cells were treated with **YHR17** (0.1, 0.3, 1, 3, 10, 33 μM) and Cisplatin (10 μM) for 48 h. Untreated cells were used as control group. The cells were trypsinized and washed three times with cold PBS, then centrifuged at 1200 rpm for 5 min. The medium was discarded, and the cells were stained for 15 min in the binding buffer using Annexin-V-fluorescein isothiocyanate (FITC) kit. Subsequently, the cells were then labeled with PI, and the apoptotic cells were evaluated using a flow cytometer (FACSCalibur BD, USA). The data were analyzed with ModFit Lt Mac V3.0.

4.8 Kinase inhibitory activities

YHR3, YHR 4, YHR 5, YHR 7, YHR 17 and 2-*epi*-jaspine B were dissolved in pure DMSO to prepare 10 mM stock solutions and diluted with Kinase buffer (pH = 7.4, composition: 40 mM/L Tris, 10 mM/L $MgCl_2$, 0.1 g/L BSA, 1 mM/L DTT, 10 μM/L ATP). SphK1/2 was added to 96-well plates, which were then treated with desired concentrations of **YHR3, YHR 4, YHR 5, YHR 7, YHR 17** or 2-*epi*-jaspine B (0.01, 0.1, 1, 10, and 100 μM) for 40 min at 30 °C. The ATP test solution was then

added, and the mixtures were incubated at room temperature for 5 min. The luminescence was immediately measured using a microplate spectrophotometer (AD 340, Beckman, USA). The data were analyzed using Graphpad Prism 5.

Conflicts of interest

There are no conflicts to declare.

Acknowledgments

We thank the National Natural Science Foundation of China (81903473 and 21801158) and the Innovation Project of Shandong Academy of Medical Sciences for the financial support.

References

[1] O. Cuvillier, G. Pirianov, B. Kleuser, P.G. Vanek, O.A. Coso, S. Gutkind, S. Spiegel, Suppression of ceramide-mediated programmed cell death by sphingosine-1-phosphate, Nature, 381 (1996) 800-803.

[2] N.J. Pyne, M. McNaughton, S. Boomkamp, N. MacRitchie, C. Evangelisti, A.M. Martelli, H.R. Jiang, S. Ubhi, S. Pyne, Role of sphingosine 1-phosphate receptors, sphingosine kinases and sphingosine in cancer and inflammation, Advances in biological regulation, 60 (2016) 151-159.

[3] A. Olivera, T. Kohama, Z. Tu, S. Milstien, S. Spiegel, Purification and characterization of rat kidney sphingosine kinase, The Journal of biological chemistry, 273 (1998) 12576-12583.

[4] H. Liu, M. Sugiura, V.E. Nava, L.C. Edsall, K. Kono, S. Poulton, S. Milstien, T. Kohama, S. Spiegel, Molecular cloning and functional characterization of a novel mammalian sphingosine kinase type 2 isoform, The Journal of biological chemistry, 275 (2000) 19513-19520.

[5] G. Xiao, Q. Wang, B. Li, X. Wu, H. Liao, Y. Ren, N. Ai, MicroRNA-338-3p Suppresses Proliferation of Human Liver Cancer Cells by Targeting SphK2, Oncol Res, 26 (2018) 1183-1189.

[6] C.T. Wallington-Beddoe, M.K. Bennett, K. Vandyke, L. Davies, J.R. Zebol, P.A.B.

Moretti, M.R. Pitman, D.R. Hewett, A.C.W. Zannettino, S.M. Pitson, Sphingosine kinase 2 inhibition synergises with bortezomib to target myeloma by enhancing endoplasmic reticulum stress, Oncotarget, 8 (2017) 43602-43616.

[7] G.T. Kunkel, M. Maceyka, S. Milstien, S. Spiegel, Targeting the sphingosine-1-phosphate axis in cancer, inflammation and beyond, Nature reviews. Drug discovery, 12 (2013) 688-702.

[8] D. Plano, S. Amin, A.K. Sharma, Importance of sphingosine kinase (SphK) as a target in developing cancer therapeutics and recent developments in the synthesis of novel SphK inhibitors, J Med Chem, 57 (2014) 5509-5524.

[9] H. Alshaker, L. Sauer, D. Monteil, S. Ottaviani, S. Srivats, T. Bohler, D. Pchejetski, Therapeutic potential of targeting SK1 in human cancers, Adv Cancer Res, 117 (2013) 143-200.

[10] L.A. Heffernan-Stroud, L.M. Obeid, Sphingosine kinase 1 in cancer, Adv Cancer Res, 117 (2013) 201-235.

[11] B. Ogretmen, Sphingolipid metabolism in cancer signalling and therapy, Nat Rev Cancer, 18 (2018) 33-50.

[12] M.R. Pitman, M. Costabile, S.M. Pitson, Recent advances in the development of sphingosine kinase inhibitors, Cellular Signalling, 28 (2016) 1349-1363.

[13] C.S. Elizabeth A. SWEENEY, Tsutomu SHIRAHAMA, Atsushi MASAMUNE,, S.-i.H.Y.I. Hideki OHTA, Sphingosine and its methylated derivative N,N-dimethylsphingosine (DMS) induce apoptosis in a variety of human cancer cell lines., International Journal of Cancer, 66 (1996) 358-366.

[14] K.J. French, R.S. Schrecengost, B.D. Lee, Y. Zhuang, S.N. Smith, J.L. Eberly, J.K. Yun, C.D. Smith, Discovery and evaluation of inhibitors of human sphingosine kinase, Cancer research, 63 (2003) 5962-5969.

[15] J. Wang, S. Knapp, N.J. Pyne, S. Pyne, J.M. Elkins, Crystal Structure of Sphingosine Kinase 1 with PF-543, ACS Medicinal Chemistry Letters, 5 (2014) 1329-1333.

[16] M.E. Schnute, M.D. McReynolds, T. Kasten, M. Yates, G. Jerome, J.W. Rains, T. Hall, J. Chrencik, M. Kraus, C.N. Cronin, M. Saabye, M.K. Highkin, R. Broadus, S.

Ogawa, K. Cukyne, L.E. Zawadzke, V. Peterkin, K. Iyanar, J.A. Scholten, J. Wendling, H. Fujiwara, O. Nemirovskiy, A.J. Wittwer, M.M. Nagiec, Modulation of cellular S1P levels with a novel, potent and specific inhibitor of sphingosine kinase-1, The Biochemical journal, 444 (2012) 79-88.

[17] V. Ledroit, C. Debitus, C. Lavaud, G. Massiot, Jaspines A and B: two new cytotoxic sphingosine derivatives from the marine sponge Jaspis sp, Tetrahedron Letters, 44 (2003) 225-228.

[18] H. Yoo, Y.S. Lee, S. Lee, S. Kim, T.Y. Kim, Pachastrissamine from Pachastrissa sp. inhibits melanoma cell growth by dual inhibition of Cdk2 and ERK-mediated FOXO3 downregulation, Phytother Res, 26 (2012) 1927-1933.

[19] C. Santos, I. Fabing, N. Saffon, S. Ballereau, Y. Génisson, Rapid access to jaspine B and its enantiomer, Tetrahedron, 69 (2013) 7227-7233.

[20] P. Ghosal, S. Ajay, S. Meena, S. Sinha, A.K. Shaw, Corrigendum to "Stereoselective total synthesis of Jaspine B (Pachastrissamine) utilizing iodocyclization and an investigation of its cytotoxic activity" [Tetrahedron: Asymmetry 24 (2013) 903–908], Tetrahedron: Asymmetry, 24 (2013) 1625.

[21] P. Ghosal, S. Ajay, S. Meena, S. Sinha, A.K. Shaw, Stereoselective total synthesis of Jaspine B (Pachastrissamine) utilizing iodocyclization and an investigation of its cytotoxic activity, Tetrahedron: Asymmetry, 24 (2013) 903-908.

[22] Y. Yoshimitsu, S. Oishi, J. Miyagaki, S. Inuki, H. Ohno, N. Fujii, Pachastrissamine (jaspine B) and its stereoisomers inhibit sphingosine kinases and atypical protein kinase C, Bioorganic & medicinal chemistry, 19 (2011) 5402-5408.

[23] G. Srinivas Rao, B. Venkateswara Rao, A common and stereoselective strategy for the synthesis of N,O,O,O-tetra-acetyl d-ribo-(2S,3S,4R)-phytosphingosine and 2-epi-jaspine B, Tetrahedron Letters, 52 (2011) 4861-4864.

[24] G. Srinivas Rao, B. Venkateswara Rao, A common strategy for the stereoselective synthesis of anhydrophytosphingosine pachastrissamine (jaspine B) and N,O,O,O-tetra-acetyl d-lyxo-phytosphingosine, Tetrahedron Letters, 52 (2011) 6076-6079.

[25] M. Martinková, E. Mezeiová, J. Gonda, D. Jacková, K. Pomikalová, Total synthesis of (−)-jaspine B and its 4-epi-analogue from d-xylose, Tetrahedron:

Asymmetry, 25 (2014) 750-766.

[26] M. Martinkova, J. Gonda, Marine cytotoxic jaspine B and its stereoisomers: biological activity and syntheses, Carbohydr Res, 423 (2016) 1-42.

[27] D. Canals, D. Mormeneo, G. Fabrias, A. Llebaria, J. Casas, A. Delgado, Synthesis and biological properties of Pachastrissamine (jaspine B) and diastereoisomeric jaspines, Bioorganic & medicinal chemistry, 17 (2009) 235-241.

[28] H. Jeon, H. Bae, D.J. Baek, Y.S. Kwak, D. Kim, S. Kim, Syntheses of sulfur and selenium analogues of pachastrissamine via double displacements of cyclic sulfate, Organic & biomolecular chemistry, 9 (2011) 7237-7242.

[29] H. Ohno, M. Honda, N. Hamada, J. Miyagaki, A. Iwata, K. Otsuki, T. Maruyama, S. Nakamura, I. Nakanishi, S. Inuki, N. Fujii, S. Oishi, Identification of selective inhibitors of sphingosine kinases 1 and 2 through a structure-activity relationship study of 4-epi-jaspine B, Bioorganic & medicinal chemistry, 25 (2017) 3046-3052.

[30] B.L. Tomoya Fujiwara, Wenqi Niu, Kazuki Hashimoto, Hisanori Nambu, Takayuki Yakura, Practical Synthesis of Pachastrissamine (Jaspine B), 2-epiPachastrissamine, and the 2-epi-Pyrrolidine Analogue, Chem. Pharm. Bull. , 64 (2016) 179-188.

Highlights

The structure-activity relationship (SAR) of tetrahydropyrrolidine analogs was established based on the MTT assay.

YHR17 exhibited potent antiproliferative activities with IC_{50} values ranging from 0.68 to 5.68 μM against tested cancer cell lines.

YHR17 has more than 125-fold selectivity for SphK1 over SphK2.